Journal of Hydrology 424–425 (2012) 124–142

Contents lists available at SciVerse ScienceDirect

Journal of Hydrology

journal homepage: www.elsevier.com/locate/jhydrol

Human induced discharge diversion in a tropical delta and its environmental implications: The Patía River, Colombia

Juan D. Restrepo [a,*], Albert Kettner [b]

[a] Department of Geological Sciences, Eafit University, AA 3300 Medellín, Colombia
[b] Community Surface Dynamics Modeling System, CSDMS, Institute of Arctic and Alpine Research, University of Colorado at Boulder, CO, USA

ARTICLE INFO

Article history:
Received 11 February 2011
Received in revised form 16 June 2011
Accepted 27 December 2011
Available online 4 January 2012
This manuscript was handled by Konstantine P. Georgakakos, Editor-in-Chief, with the assistance of Ellen Wohl, Associate Editor

Keywords:
Patía River
Hydrologic alteration
River diversion
Sediment load
Deltas
Coastal environmental change

SUMMARY

The Patía River, the number one in terms of sediment yield ~1500 t km^{-2} yr^{-1} draining the western South America, has the most extensive and well developed delta on the Pacific coast, measuring 1700 km^2. During the Holocene, nature forced the Patía delta to the south; however, a major water diversion, starting in 1972, diverted the Patía flow to the Sanguianga River, the latter, a small stream draining internal lakes from the Pacific lowlands. This human induced discharge diversion shifted the active delta plain back to the north and changed the northern estuarine system into an active delta plain. Overall, major environmental consequences of this discharge diversion in terms of morphological changes along the delta coast and distributary channels, are evidenced by: (1) coastal retreat along the abandoned delta lobe; 63% of the southern shoreline is retreating at maximum rates of 7 m yr^{-1}, with a corresponding coastal land loss of 106 m yr^{-1}; (2) transgressive barrier islands with exposed peat soils in the surf zone; (3) abandonment of former active distributaries in the southern delta plain with associated closing of inlets and formation of ebb tidal deltas; (4) breaching events on barrier islands; and (5) distributary channel accretion in the northern delta plain by morphological processes such as sedimentation (also in crevasses), overbank flow, increasing width of levees, interdistributary channel fill, and colonization of pioneer mangrove. The Sanguianga Mangrove National Park (SMNP), the largest mangrove reserve in Colombia, measuring 800 km^2, lies in this former estuary, where major hydrologic and sedimentation changes are occurring. Observed environmental changes in the SMNP, include (1) seaward advance of the sub-aqueous delta front at the Sanquianga inlet evidenced by an increase in tidal flat area from 5.4 Mm^2 in 1986 to 14 Mm^2 in 2001; (2) freshening conditions in the Sanguianga distributary channel, a hydrologic change that has shifted the upper estuarine region (salinity <1 psu) downstream; (3) downstream advance of freshwater vegetation, which is invading channel banks in the lower and mixing estuarine zones; (4) die-off of approximately 5200 ha of mangrove near the delta apex at Bocas de Satinga; and (5) recurrent periods of mangrove defoliation due to a warm plague. Further analysis indicate that during the past two decades, processes such as mangrove erosion in the delta shore, are the result of a short-term relative sea-level rise of 5.1 mm yr^{-1} for the 1984–2006 yr-period, after the devastating tsunami of 1979. In the Patía catchment, erosion rates have been more pronounced during the 1970–1980 and 1990–2000 decades, as a result of land degradation and deforestation. Preliminary results indicate that relative resent anthropogenic influences on the Patía River drainage basin have altered the deltaic environment and beyond significantly.

1. Introduction

Natural and human-induced factors that control the evolution of delta environments vary in time and space (Galloway, 1975; Ashton et al., 2001; Penland and Kulp, 2005; Day and Giosan, 2008; Syvitski et al., 2009). For example, various distributary systems of any given delta may be differentially influenced by river discharge, sea level rise, wave action and tides (Restrepo et al., 2002; Syvitski et al., 2009). Also, anthropogenic influences, including direct impacts affecting river discharge and sediment load such as water diversion, deforestation, dam emplacement and water diversion for irrigation alter the morphology of deltaic systems (IPCC, 2001; Hood, 2010). Thus, a study on how delta systems respond to both natural and human induced forces necessarily requires a sufficient knowledge of the system's functioning, both for natural (physical and biological) and human components and corresponding interactions. In addition, during the implementation of management strategies in any particular system during a

* Corresponding author. Address: Cra 49 No. 7 sur 50, Eafit University, Medellín, Colombia. Fax: +57 4 2664284.
E-mail address: jdrestre@eafit.edu.co (J.D. Restrepo).

0022-1694/$ - see front matter © 2011 Elsevier B.V. All rights reserved.
doi:10.1016/j.jhydrol.2011.12.037

specific time period, requires analyzing and determination of the key controlling factors that act on that specific delta (e.g. Ericson et al., 2006).

Delta aggradation has been widely reduced due to the reduction of active distributary channels to support navigation and elaborated irrigation systems. Major deltas such as Magdalena, Nile, Vistula, Yellow and Indus have experienced a considerable decrease in their distributary channel number and therefore in their aggradation rates (Syvitski et al., 2009).

Deltaic river distributary channels often changed episodically their location and pattern due to natural forces during the Holocene – pre-Anthropocene; causing further aggradation of delta lobes (Syvitski et al., 2009). Along the Pacific coast of Colombia (Fig. 1A), the overall southward displacement of the main delta distributary channels have been associated with the presence of active transcurrent faulting associated with several transverse paleofracture zones (Gómez, 1986a,b; Correa, 1996; González et al., 2002; Restrepo et al., 2002) (Fig. 1B). Paleochannels indicate that delta distributaries have undergone rearrangements due to seismic events (Gómez, 1986a). Tectonic activity in the Pacific deltas of Colombia caused that most of the active distributaries switched their locations from northerly to southerly over the course of 50 decennia (Restrepo et al., 2002).

For the Patía River delta (Fig. 1), the largest and best-developed delta on the western margin of South America, geologic indicators provide evidence that the active delta lobe shifted to the south 500 years ago (Correa, 1996) where it stayed until recently. The northern part became an estuarine system characterized by large extensions of mangrove ecosystems, little fresh water inflow and no significant fluvial sediment inflow from the western Andes. The Sanquianga Mangrove National Park (hereafter named SMNP) is the largest ecological reserve along the Pacific coast South America and is situated on this former active delta plain (Fig. 1D).

During the early seventies the deltaic system altered dramatically as a wood merchant constructed a 3 km-long channel (Canal Naranjo), which was dredged to connect the Patía Viejo distributary with the much smaller Sanquianga River to the north (Fig. 1D). This channel was constructioned to transport wooden logs more easily from the Patía Viejo distributary to the Sanquianga River by means of a winch, where most of the sawmills were located at that time. Riverbank failure caused severe flooding, triggered by a La Niña storm event in 1973, and started to widening the Canal Naranjo. Discharge diversion, which started during the flooding event, became even more pronounced during an additional flood in 1977 (National Report of Defensoría del Pueblo).

Prior the construction of Canal Naranjo in 1972, the Patía Viejo distributary channel joined the Patía River at Fátima whereafter the fluvial flow continued its course towards Salahonda, the then active delta lobe in the southern part of the delta plain. Post 1973 flooding event, the Sanquianga River, which use to be a small creek draining mostly small internal lakes (Fig. 1D), started to increase its water discharge from approximately 50–1500 $m^3 s^{-1}$; a 30 times increase! After 1990, more than 80% of the Patía River discharge was redirected through the Canal Naranjo – Patía Viejo distributary – to the Sanquianga River system. This diversion left the southern delta plain under sediment starving conditions and reduced the fresh water flow by more than a magnitude. Presently the Sanquianga River passes Bocas de Satinga to the north (Fig. 1D), carring more than 90% of the Patía River flux northwards (Bateman et al., 2009).

This paper presents how anthropogenic forces altered the flow direction of the Patía River, which shifted the active delta plain from the south to the north, changing the northern estuarine system into an active river delta. We analyze the environmental consequences of this discharge diversion in terms of (1) morphological changes along the delta front and distributary channels, (2) ecological impacts on mangrove ecosystems, (3) changes in fishing resources, and (4) social implications to villagers of the Patía delta. We also discuss likely long-term impacts of this channel diversion to the coral reef formations of Gorgona Island, a tropical Pacific coral reef located in the pathway of the Sanquianga River delta (Fig. 1D).

According to the scientific program of dynamics and vulnerability of river delta systems, run by the Community Surface Dynamics Modeling System Group, University of Colorado, and sponsored by GWSP (Global Water System Project) and LOICZ (Land Ocean Interaction in the Coastal Zone, a core project of the IGBP) (Overeem and Syvitski, 2009), the information presented here is a valuable tool to: (1) craft a science and implementation plan for a joint assessment and synthesis research project on vulnerability of deltas, based on input from an interdisciplinary group of experts, scientists, and decision-makers of the earth system; (2) enhance a prototype global database of river delta systems featuring status and scenarios of change and options for adaptation; and (3) to identify key research questions and challenges for sustainable development to which the integrated database and subsequent analysis and modeling could be applied.

2. The Patía River delta

The morphology and recent evolution of the Colombian deltas are unique compared to other South American deltas because of the singular combination of extreme climatic, geological, and oceanographic conditions in which the deltas are built, including (1) high tectonic activity with the occurrence of shallow earthquakes and tsunamis (Kellogg and Mohriak, 2001); (2) active margins characterized by narrow continental shelves with limited accommodation space (Correa, 1996) (Fig. 1A); (3) drainage basins that receive high rates of precipitation resulting in large quantities of water discharge and sediment load (Restrepo and Kjerfve, 2000); (4) the complexity of littoral dynamics resulting from micro and mesotidal ranges (Restrepo and Kjerfve, 2002; Restrepo et al., 2002), and the effect of significant swells and associated coastal currents (Restrepo et al., 2002); (5) strong oceanographic manifestations associated with the ENSO cycle, causing sea level rises during El Niño years (Morton et al., 2000); and (6) increasing rates of relative sea level (Restrepo et al., 2002; Restrepo and López, 2008). It is worth noting that small rivers form extensive deltas along the Pacific Colombian coast, even under the occurrence of high energetic and destructive conditions of the ocean.

The Patía (Fig. 1), a littoral barred delta with a sub-aerial area of $\sim$1700 km^2, consists of distributary channels flanked by tropical humid forests, mangrove swamps, tidal flats, and barrier islands. The delta is characterized by high tectonic activity and progrades on a narrow shelf bordering a deep trench. Along the Colombian Pacific margin, the Nazca oceanic plate is converging with the South American continental plate at a rate of 54 mm yr^{-1} (Kellogg and Mohriak, 2001) (Fig. 1A). The convergence has produced an unstable coast characterized by the occurrence of large magnitude and shallow focus earthquakes. Severe earthquakes, accompanied by destructive tsunamis that impacted the Patía River delta are recorded in 1836, 1868, 1906 and 1979 (Pennington, 1981; Lockridge and Smith, 1984; Meyer et al., 1992).

According to Restrepo and López (2008), the Patía delta is a tide-influenced system and exhibits definite characteristics of mixed wave and tide-influenced delta due to the interplay of (1) moderate wave conditions as a result of the effect of significant swells from the SW; (2) meso-tidal ranges; (3) a steep subaqueous profile; and (4) a low attenuation index of deep-water waves. As a result, marine energy conditions of the Patía delta are one of the highest of all Colombian deltas (marine power of 9.1), more

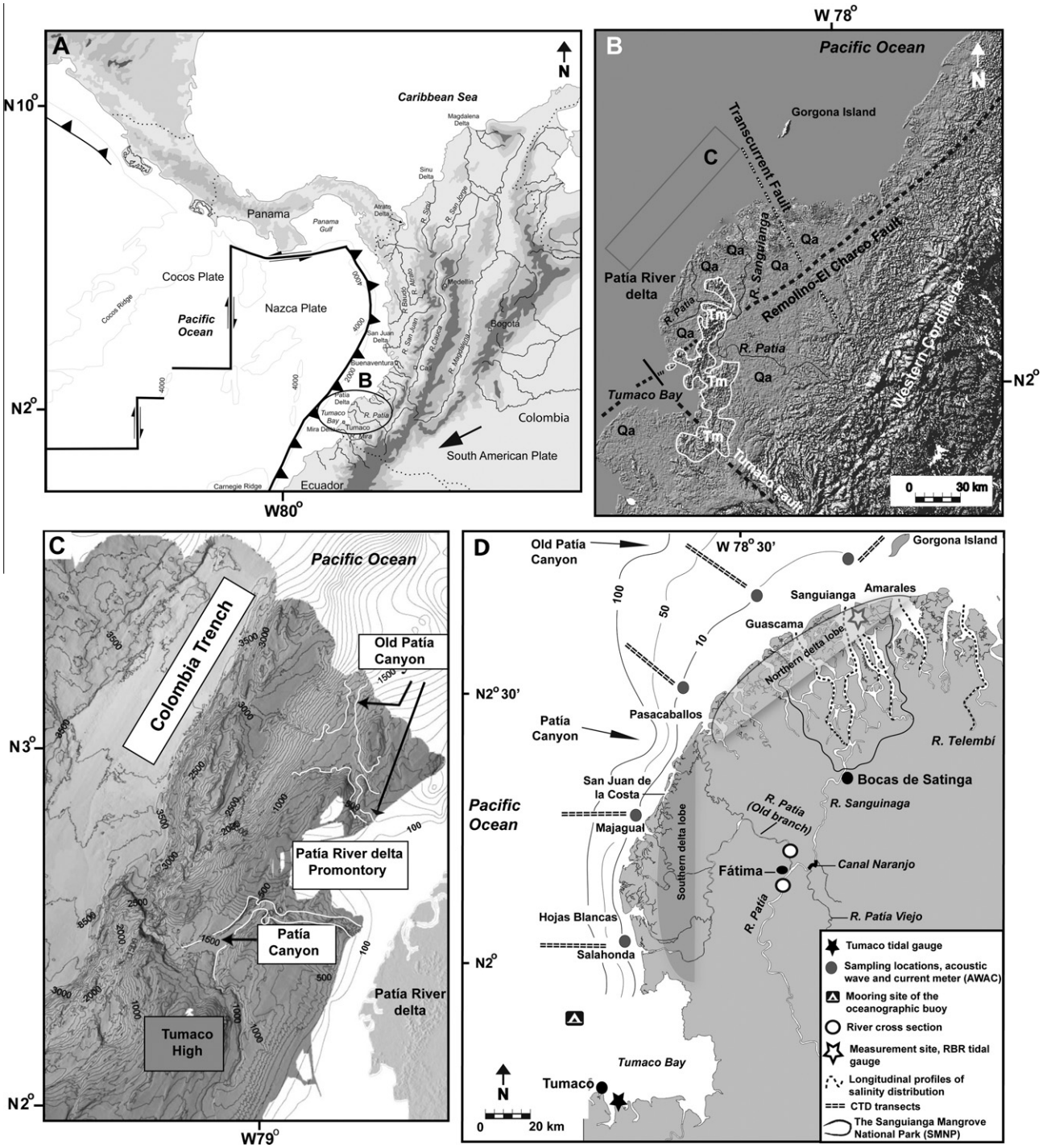

Fig. 1. (A) Map of the Pacific coast of Colombia, showing the tectonic setting of the Pacific active margin. (B) Hillshade generated from DEM data (SRTM, Shuttle Radar Topography Mission, 2002), showing the main tectonic features and geologic formations of the Patía River delta, including transverse paleofractures, recent alluvial deposits (Qa), and Tertiary formations of marine Miocene rocks (Tm). (C) Major bathymetric features in front of the Patía delta promontory, including the old canyon in the northern delta lobe and the current canyon in the southern delta front (Modified from Collot et al., 2005). (D) Map of the Patía River delta, showing the locations of: (1) the channel diversion site at Fátima, (2) southern and northern delta lobes, and (3) sampling locations of oceanographic and hydrologic measurements.

comparable to the large deltas bordering the Atlantic ocean of South America such as the Orinoco and the Paraná deltas. Overall, recent evolution of the Patía delta has been affected by a combination of factors: (1) high rates of rainfall (4700 mm yr^{-1}) in the hinterland of the drainage basin, which results in high fresh water discharge and sediment yield (1500 t km^{-2} yr^{-1}); (2) low discharge variability (Q_{max}/Q_{min}); (3) a relative sea-level rise of 5.1 mm yr^{-1} after the occurrence of the 1979 tsunami; (4) ongoing high tectonic activity in the receiving basin; (5) the occurrence of non-storm overwash on barrier islands associated with ENSO sea-level anomalies; and (6) the spatial switch of delta distributaries related to tectonic induced subsidence and human impacts.

The Patía delta is situated along the southern part of the Colombian Pacific coast, just north of the Tumaco Bay (Fig. 1B). The Tumaco Bay-Patía deltaic area is located on the Tumaco segment (Orozco, 2004), which is the southernmost portion of the Atrato-Tumaco

terrain (Etayo-Serna, 1983). The region is dominated by a Miocene sedimentary belt of marine successions of sandstones, siltstones and claystones of the Guapi and Naya formations (Correa and González, 1988). This sedimentary belt has a NNE regional trend and extends from Buenaventura Bay, where it is covered by recent alluvial sediments and tilted towards the west, to near Tumaco Bay, where it is more compressed and uplifted. From the delta plain to the basin's upper reaches, the area is characterized by Plio-Pleistocene fluvial-volcanic and massive Cretacic volcanic-sedimentary sequences and andesitic lavas produced by the recent volcanism of the Western Cordillera (Arango and Ponce, 1982).

Along the coastal zone, the sedimentary belt is expressed in a series of NNE-oriented structures that gradually decrease in relief north of Tumaco Bay. South of Buenaventura (Fig. 1A) the Cenozoic rocks lay sub-horizontally without any marked compressing effects that could produce narrow folding (Gómez, 1986a). In contrast, the faulting and folding of the sedimentary sequence south from the Patía River delta have produced a series of hills with Tertiary rocks of the Guapi and Naya formations (Arango and Ponce, 1982; Gómez, 1986a) (Fig. 1B). In the area, transcurrent faults parallel to the coastline have been documented, including the Buenaventura and the Naya-Micay, both located to the north of the Patía delta, and the Remolino-El Charco fault within the Tumaco Bay (Arango and Ponce, 1982; Gómez, 1986b; Cediel et al., 2003). This active transcurrent faulting has been associated with several transverse Cretaceous paleofracture zones (Case et al., 1971), including the Tumaco fault (Gómez, 1986a) and the paleofracture in the northern part of the Patía delta. The latter coincides with a submarine canyon at the Sanquianga mouth (Fig. 1B and C).

Located in the northern Patía River delta, the Sanquianga Mangrove National Park (SMNP), a highly productive ecosystem, is now part of the active delta plain. The mangrove complex, covering an approximate area of 800 km^2, comprises a large estuarine system from the current delta Gómezapex at Bocas de Satinga to the coast (Fig. 1D). More than 7000 people are dependent on the SMNP for fisheries and wood resources. Fisheries have traditionally exploited species like Piangua (*Anadara tuberculosa* and *Anadara similis*), white shrimp (*Litopenaeus occidentalis*), tiger shrimp (*Litopenaeus vanamei*, and tití shrimp (*Xiphopenaeus riverti*), which account for more than 70% of the annual catch in weight and in number of individuals. However, during the last 30 years, the discharge diversion of the Patía River have profoundly modified the entire SMNP, leading to a general degradation of the ecosystem and to a substantial decrease in the abundance of fauna. The diversion of the Patía to the Sanquianga River through the Canal Naranjo (Fig. 1D) has increased freshwater runoff and sediment load. The modification of hydrologic patterns and sedimentation processes in the SMNP has induced a gradual decrease in salinity and an increase in total suspended solids, altering the composition, distribution, zonation, and abundance of vegetation and fauna. For instance, the total annual catch of Piangua, *A. similis*, a mollusk highly vulnerable to changes in salinity, has decreased 90% in the last 15 years. In addition, changes in longitudinal gradients of salinity are altering the zonation of mangroves. Currently, woody species that favor freshwater and brackish conditions are invading riverine mangroves, changing the entire community structure. The recent environmental degradation of the SMNP ecosystem has had severe economic and social implications for the region (Tavera, 2009).

3. Data and analysis

Daily water discharge and suspended sediment load data (1969–2003) were obtained at 4 sites along the Patía River from the Hydrological Institute of Colombia, IDEAM (IDEAM, 2009) (Fig. 2). In addition, we took measurements of water discharge at two river cross-sections in the apex of the delta at Fátima during December 2009 (Fig. 1D). Water discharge measurements were obtained using the AWAC velocity profiles. The measurements and cross-sectional integration were done following the USGS routine (Buchanan and Somers, 1969). Morphometric variables (drainage basin area, relief and longitudinal profile) of the selected tributary catchments of the Patía basin were obtained from Shuttle Radar Topography Mission data 3 arc sec horizontal and 1 meter vertical resolution, with an uncertainty ranging from ±1.1 to 2 m in the lowlands to ±6 m in the highland regions (Farr et al., 2007; Berry et al., 2007). River network pattern were explored to assess patterns of sediment retention throughout the river network. Basin-averaged temperature and precipitation data were assessed using HidroSig Java (version 1.8) climate archives (HIDROSIG, 2006), which include all existing hydrological and meteorological databases of Colombia.

To assess morphological changes along the delta front and distributary channels during the last four decades, after the channel diversion occurred in 1972, 30 m pixel resolution Landsat 7 satellite images from 1986, 1987, 1996 and 2001 were processed, obtained from the Global Land Cover Facility of the University of Maryland. The images were rectified to 1:25,000 topographical maps (Geographic Institute of Colombia, IGAC) after establishing ground control points. The geo-registered images were corrected for atmospheric path radiance by subtracting band minimum values from within the darkest topographic shadows. Detailed temporal analyzes of distributary channel morphology at the diversion site and shoreline changes along the delta front were documented using aerial photographs from 1962 and 1986 at scale 1:40,000, topographic maps at scale 1:25,000, and through interviews with inhabitants. In addition, we analyzed how delta morphology has changed during the past century by using a French Navy chart from 1875 and a local map from 1924.

To estimate rates of coastal retreat and progradation, the coastline was extracted from satellite images in 1986 and 2001 by using ISODATA and band ratio methods. The coastline rate of change was determined by using DSAS software, which estimates rate of change statistics from multiple historic shoreline positions residing in GIS (Thieler et al., 2005). DSAS transects were spaced 100 m apart and rates of shoreline change were calculated at each transect using linear regression applied to both shoreline positions in 1986 and 2001. A hypothetical baseline was defined according to shoreline orientations. All analyzed images correspond to low tide conditions, so variance in the shoreline location that might be interpreted as coastal erosion or accretion due to the mesotidal range, that is so characteristic for the Patía delta, can be neglected.

Field observations were carried out along five main distributaries and their inlets, Sanquianga, Guascama, Pasacaballos, Majagual and Salahonda, to compare and contrast the physical changes occurring in the delta distributaries and associated coastal areas. Additional measurements at six stations along the delta front, south from the main current distributary channel, the Sanquianga River and its inlet were obtained. The measurements consisted of (Fig. 1D):

1. Time series observations of currents, wave parameters, and water level elevation at six stations in the Patía delta front using two Nortek acoustic wave and current meters AWAC (including pressure sensors with a resolution of 0.25%). The instruments were programmed to calculate a 5 s average every 10 min, deployed at the center of each navigational channel and maintained 1 m above the bottom. At the coastal zone, the AWACs were installed at ~10 m depth. All observations were made during complete tidal cycles in July and December 2009 and November 2010.

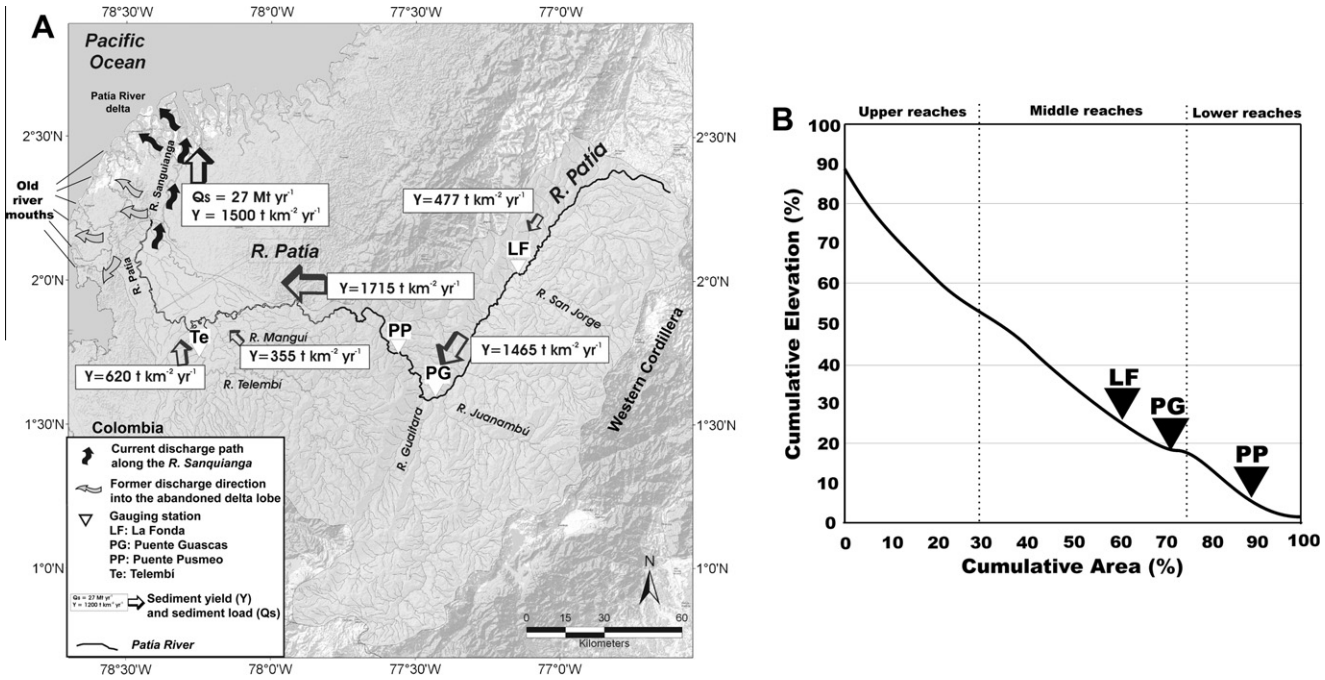

Fig. 2. (A) Map of the Patía River drainage basin, showing the principal tributaries, the four hydrological stations (triangles) where water discharge and sediment load are gauged, and the mean annual sediment load values at the upper, middle and lower reaches of the Patía River (arrows). (B) Longitudinal profile of the Patía River, showing the location of main hydrological stations. It is worth noting the limited alluvial plain to trap sediments.

2. Time series measurements of water-level elevation at a single station in the Sanquianga River mouth using a RBR tidal gauge. The instrument was programmed to estimate water levels every 20 min, and remained moored for 32 days, starting on 23 June 2010.
3. Conductivity, temperature and depth (CTD) measurements were made along profiles up to 20 km seaward of the delta front mouth at a maximum depth of approximately 60 m, to investigate the stratification of water masses and plume front dynamics. These CTD casts were taken using a Seabird CTD moored on a winch on the research vessel during December 2009 and November 2010. Each longitudinal transect was started at the middle of the ebb tide at each distributary entrance, and ended at the low tide at the seaward end of the transect. Also, MODIS imagery from Moderate Resolution Imaging Spectroradiometer onboard NASÁs Aqua and Terra satellites, were analyzed to assess river floods, in situ flooding, and plume dispersion along the delta front.
4. Longitudinal measurements of vertical profiles of conductivity and temperature were taken along the Sanquianga distributary channel from the entrance to the apex at Bocas de Satinga to obtain a quasi-synoptic characterization of the longitudinal salinity distribution. These measurements were made during June 2010 using a YSI-CTD CastAway profiler.

In addition, hourly sea level data were obtained from the tidal gauge at Tumaco (1953–2006) (Fig. 1D). The sea level data is approximately 94% complete and missing data are interpolated with harmonic analysis (Franco, 1988, 1992). The trend in relative sea level in the Patía delta is estimated by least-squares linear regression for the Tumaco time series. To evaluate the monthly mean sea level anomalies near the deltas related to ENSO, we removed mean monthly values to eliminate seasonal effects. A filtered sea level was calculated by subtracting the interannual mean sea level for each month (S^*) from the respective monthly mean sea level in each year (S) for the ith month of the jth year to form the deviation from the long-term monthly mean sea level $S_{ij} = S_{ij} - S_i^*$ (Quinn et al., 1978; Enfield and Allen, 1980). The Sea Surface Temperature anomaly (SST) data were obtained from the National Oceanic and Atmospheric Administration-NOAA.

Seasonal and interannual variability of wave climate conditions along the Patía delta were assessed from wave data for the 1978–2001 period from the NOAA implementation of the third-generation wind-wave model WAVEWATCH III (NWW3). The NWW3 predicts the evolution in the two-dimensional physical space and time of the wave action density spectrum as a function of the wave number and direction (Tolman, 2002). The type of output used in this study consists in full spectral data at selected output points within the southern Pacific coast of Colombia. The data include 84,552 sets of predominant direction, significant height, and peak period. Also, we obtained wave data along the delta front from the AWAC measurements, including significant and maximum wave heights, peak and mean wave periods, and wave direction. Further wave information was obtained from May 2008 to October 2009 by deploying an oceanographic buoy in the southern part of the delta (Fig. 1D).

4. Results

4.1. Water discharge and sediment load into the delta plain

The Patía River catchment with an area of 23,700 km^2 has the largest drainage basin of the Colombian Rivers draining into the Pacific. Based on daily stage measurements from 1969 to 2003, the Patía River as gauged at Puente Pusmeo (Fig. 2A) discharges on average 10 km^3 yr^{-1}, with a seasonal root mean square (rms) of 3 km^3 yr^{-1}. Peak flows exceeding 14 km^3 yr^{-1} are observed during La Niña years 1973, 1984, and 2000, while low discharges below 9 km^3 yr^{-1} are observed during El Niño years 1972 and 2001 (Fig. 3A). The mean river discharge flowing into the delta plain is 42 km^3 yr^{-1} because of the large contribution of the Telembí River, the last tributary before the delta (Fig. 2A).

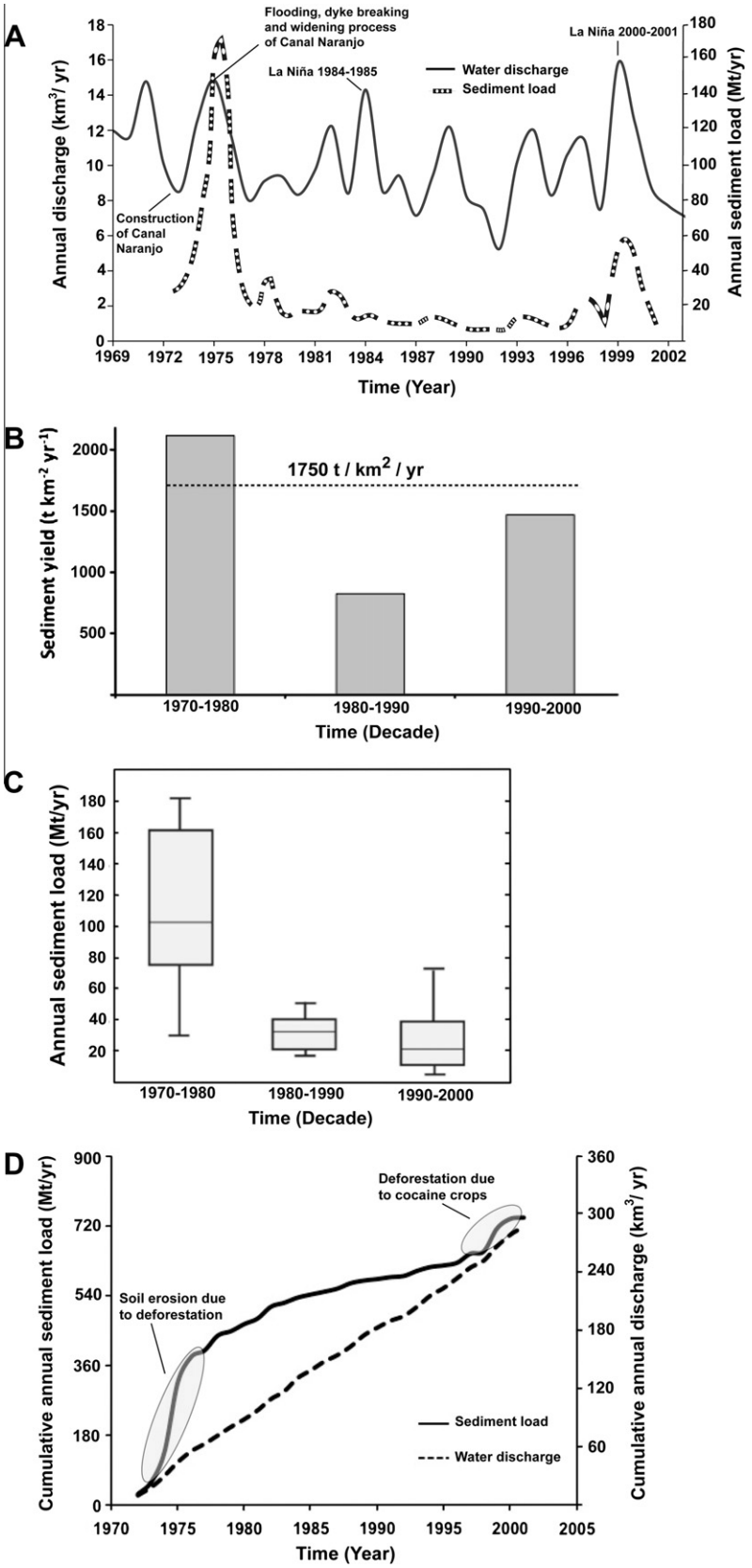

Fig. 3. Water discharge and sediment load variability for the Patía River at Puente Pusmeo. (A) Plots of river discharge data for the 1967–2002 year-period and annual sediment load for the 1972–2001 year-period (dotted line). (B) Decadal variability of sediment yield. (C) Box-whisker plots annual sediment yield during the three analyzed decades in the lower reaches of the Patía River, showing the medians, 25th percentiles, 75th percentiles. (D) Plot of cumulative suspended sediment load and cumulative annual water discharge. The location of the hydrological station at Puente Pusmeo is shown in Fig. 2A.

Based on daily sediment load data from 1972 to 2001 by IDEAM, sediment loads from the upper river measure 0.92, 16.2, and 13.9×10^6 t yr^{-1}, gauged at La Fonda, Puente Guascas, and Puente Pusmeo, respectively (Fig. 2B). The corresponding sediment yield ranges from 477 t km^{-2} yr^{-1} at La Fonda to 1715 t km^{-2} yr^{-1} at Puente Pusmeo for the most downstream portion of the river (Fig. 2A). The latter yield, which represents 60% of the whole catchment area, does not express the conditions of deposition and storage that occur in the entire basin. To remedy this, we further estimated sediment load for the non-gauged area of the Patía River from the regression of sediment yield on basin area from gauged stations. The mean sediment yield for the watersheds of Telembí and Magui rivers are 620 t km^{-2} yr^{-1} and 355 t km^{-2} yr^{-1}, respectively. Our best estimate of sediment load into the Pacific Ocean from both gauged and non-gauged Patía tributaries is $\sim 27 \times 10^6$ t yr^{-1} (Fig. 3B). This results in a sediment yield of $\sim$1500 t km^{-2} yr^{-1} for the entire basin (Fig. 2A).

The Patía River shows high decadal variability in sediment yield (Fig. 3B). Between 1972 and 1980, average sediment yield was 2200 t km^{-2} yr^{-1}. One of the human induced drivers of this high sediment yield is deforestation. Since the 1960s, the Colombian government gave many licenses to big timber log companies such as Cartón de Colombia and Maderas Pizano, among others, to remove the forests in the Patía drainage basin and its delta. According to the National Department of Statistics (Dane, 2003), 60% of the wood production in the country during the 1970s came from the Patía region. In contrast, the average sediment yield decreased to 825 t km^{-2} yr^{-1} during the 1980s. Since most of commercial forests in the catchment were removed, many sawmills went out of business. There were more than 40 sawmills during the seventies In Bocas de Satinga, along the Sanquianga River (Fig. 1D). Nowadays, only two sawmills are still active. After depleting most of the wood resources, an economic down was evident in the region. Since 1991, the average sediment yield has increased to 1470 t km^{-2} yr^{-1} (Fig. 3C). Most likely the expansion in area of deforestation due to the increase in cocaine crop plantations in the Patía catchment and its main downstream tributary, the Telembí River (United Nations Report, 2009), has increased the sediment yield (Fig. 3B).

The statistical parameters of annual sediment yield during the three analyzed decades in the lower reaches of the Patía River are shown in a box-whisker plot (Fig. 3C). The medians, 25th percentiles, 75th percentiles, and maximum values indicate high decadal variability during the 1970–1980 and 1990–2000 yr-periods as well. In fact, the temporal sediment pattern for each decade is quite different, as discussed above. A double mass plot of cumulative suspended sediment load versus cumulative annual water discharge for the Patía River shows the trend of sediment flux relative to that of water discharge (Fig. 3D), to confirm if shifts in trends of sediment load are due to changes in the flow regime or due to human-induced factors. The analysis suggests that the increase in sediment flux for the Patía commenced in the mid-1970s and its progressive steepening in the mid-1990s further indicates that the impact of land use change and intensification is increasing.

4.2. Channel diversion in the Patía River

Fig. 4 shows the morphological variations of the Patía and Sanquianga Rivers at the diversion site over time. In 1962, there was not any connection between both rivers (see number 2, Fig. 4) and the Patía Viejo was an active and meandering distributary channel. In 1978, after the Canal Naranjo was excavated, the Patía migrated towards the Sanquianga River. At this time, the Patía Viejo was an active branch with flow connection to the Sanquianga River. In 1986, the bifurcation continues actively (see number 1, Fig. 4), but the channel width indicates that discharge is approximately shared half and half. In 1997, however, the Patía River shows less hydraulic capacity and sediment accumulation creates elongated bars at the entrance of the lower part of the Patía River. The new branch, now formed by the Patía and Sanquianga, named in the region Patianga, becomes the dominant river. Currently, the Patianga transports nearly all water discharge and its width is of the same magnitude as the former Patía River width.

In addition, tectonic activity in the Patía River's drainage basin along an active fault increased the discharge diversion of the Patía River even more as a result of the 1979 earthquake. Due to the 1979 seismic event, there was a vertical displacement that resulted in the Sanquianga River to capture approximately 70% of the Patía River's discharge (Soeters and Gómez, 1985; Velásquez et al., 1994).

Fig. 5 shows cross profiles at the confluence of the Patia and the Sanquianga Rivers based on space shuttle radar topography mission (SRTM) elevation data obtained at 2002, which has a $\sim$90 m horizontal and a 1 m vertical resolution. Cross profiles A & B reflect the elevation of the abandoned Patia River stretch whereas cross profiles C & D provide elevation data of the Sanquianga River. Cross profiles of the SRTM elevation data indicates that the land and freshwater surface of the partly abandoned Patia River are located slightly higher (7 m) than the Sanguianga cross profiles, indicating that the hydraulic capacity of the Sanquianga is even more pronounced. After 1987, more than 80% of the Patía River discharge was redirected through the Canal Naranjo – Patía Viejo distributary – to the Sanquianga River system (Fig. 4). This discharge diversion left the southern delta plain under sediment starving conditions and altered the fresh water inflow to a more reduced magnitude. Presently, the Sanquianga River, discharging into Bocas de Satinga to the north (Fig. 1D), now carries more than 90% of the Patía riverine flux (Bateman et al., 2009).

Our field measurements of water discharge at the Patía River cross-section during December 2009 (Fig. 1D) show that the average water discharge before the diversion site in Fátima is $\sim$1000 m^3 s^{-1}. Further measurements indicate that a small fraction of water discharge, only 54 m^3 s^{-1} flows to the old Patía branch, confirming that the Sanquianga River presently captures almost the entire Patía River flow. It is worth noting that measurements were obtained at the beginning of rising flow levels in December, a period that coincides with the rain season of the Patía River drainage basin.

4.3. Morphological changes during the 1875–1962 yr-period

Along the Pacific coast of Colombia, the overall southward displacement of the main delta distributary channels has been associated with the presence of active transcurrent faulting associated with several transverse paleofracture zones (Fig. 1B). Paleochannel relics also suggest that delta distributaries have undergone rearrangements due to seismic movements. Tectonic activity in the Pacific deltas of Colombia caused that most of the active distributaries switched their locations from northerly to southerly.

For the Patía delta (Fig. 6), the active delta lobe shifted to the south in the Holocene, probably as a result of tectonic activity. Since then, the accreting delta front is located in the southern portion of the delta plain. The northern part became an estuarine system characterized by large extensions of mangrove ecosystems, little fresh water inflow and no significant fluvial sediment load from the western Andes.

Remainders of a paleocanyon in the Patía delta suggest that the main channel of the Patía River was located at the northern delta lobe (Fig. 1C). Transcurrrent faulting associated with several transverse paleofracture zones, including the Tumaco fault and the Patía River alignment (Fig. 1B), may have influenced the discharge displacement from the northern distributary emptying into Bocas de Satinga to the Old Patía branch (Fig. 6C). Analysis of the delta

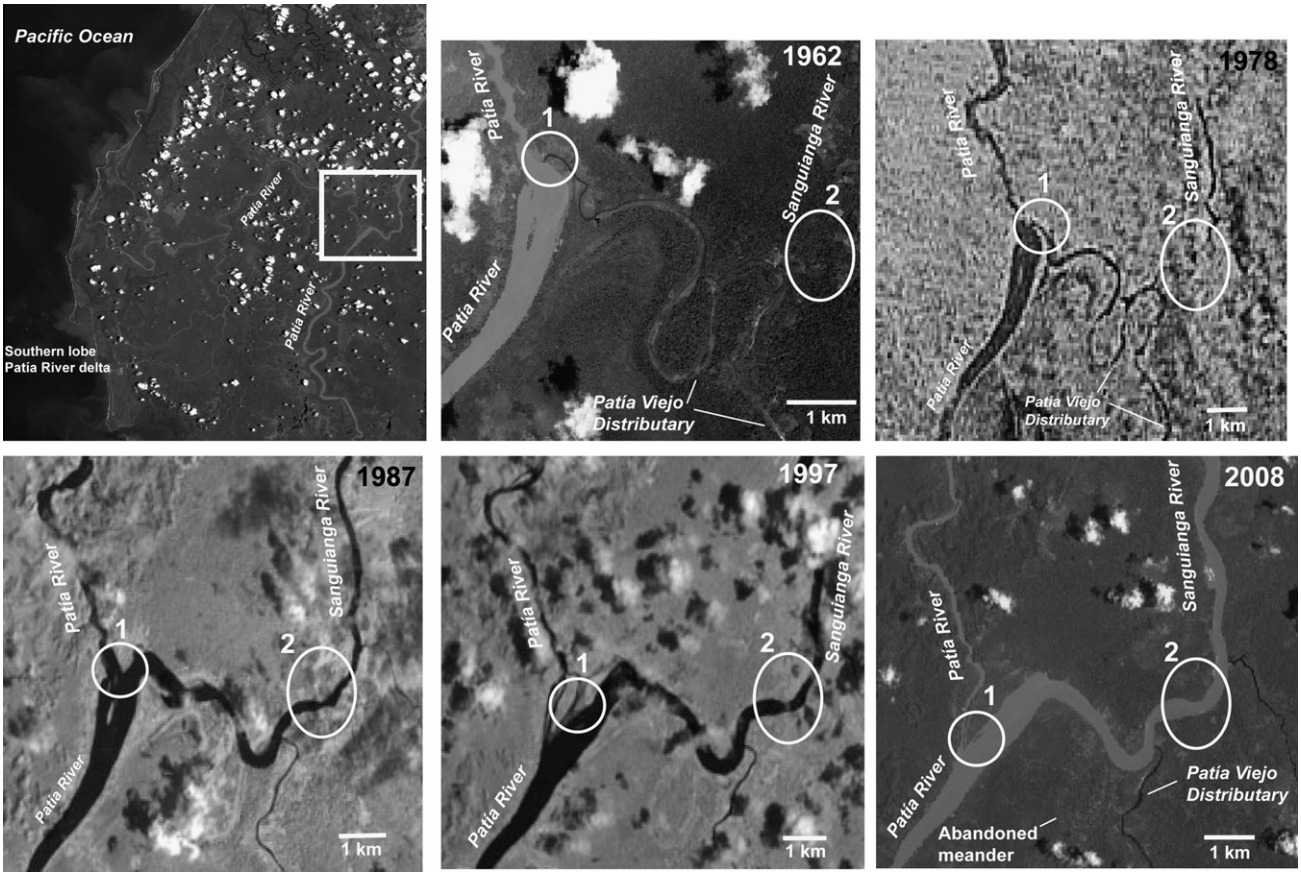

Fig. 4. Aerial photographs 1962–1978, Landsat satellite images 1987–1997, and Aster image from 2008, showing major morphological changes at the channel diversion site. Observe the widening process of the Sanquianga River and the confined flow of the Patía.

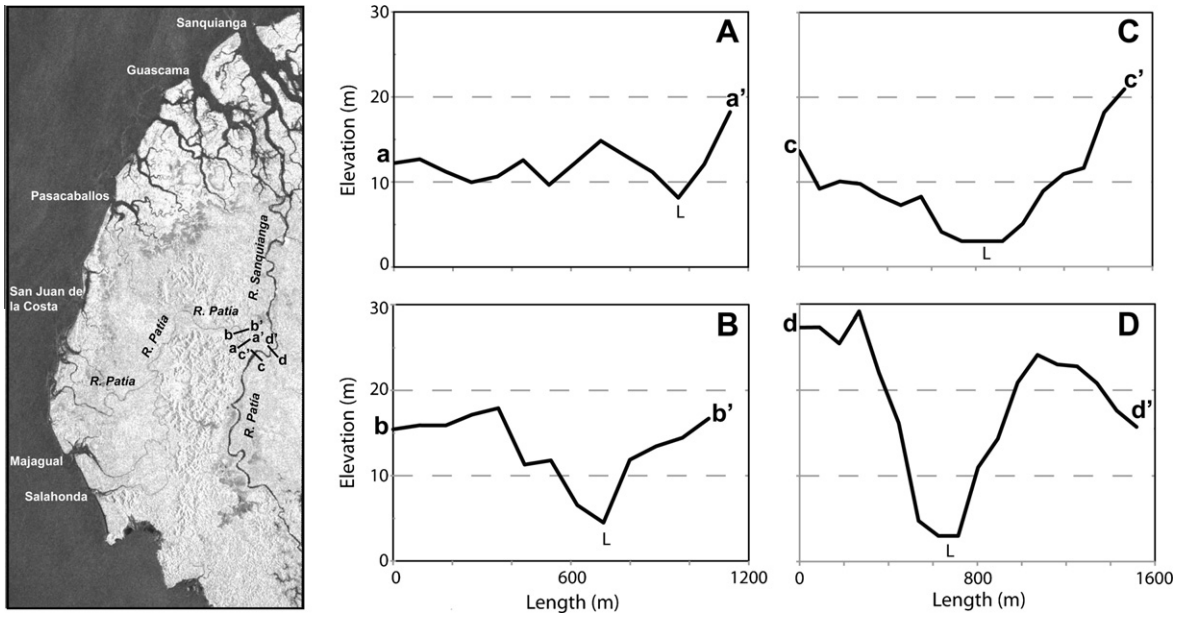

Fig. 5. River-cross profiles obtained from 1 m vertical intervals of Space Shuttle Radar (SRTM) data at the lower reaches of the Patía River. (A and B) Cross profiles reflecting the elevation of the abandoned Patia River stretch whereas. (C and D) Cross profiles providing elevation data of the Sanquianga River. The letter "L" is added to each figure to indicate where the crossings with the river are.

between 1875 and 2001 indicate significant morphological changes during this 126-year period (Fig. 6), including: (1) flow diversion from the Patía River to the Sanquianga River; (2) widening of the Sanquianga River; (3) narrowing of the Old Patía branch due to confined fluvial flows; (3) distributary channel abandonment at the former delta apex; (4) narrowing of inlets at the southern delta

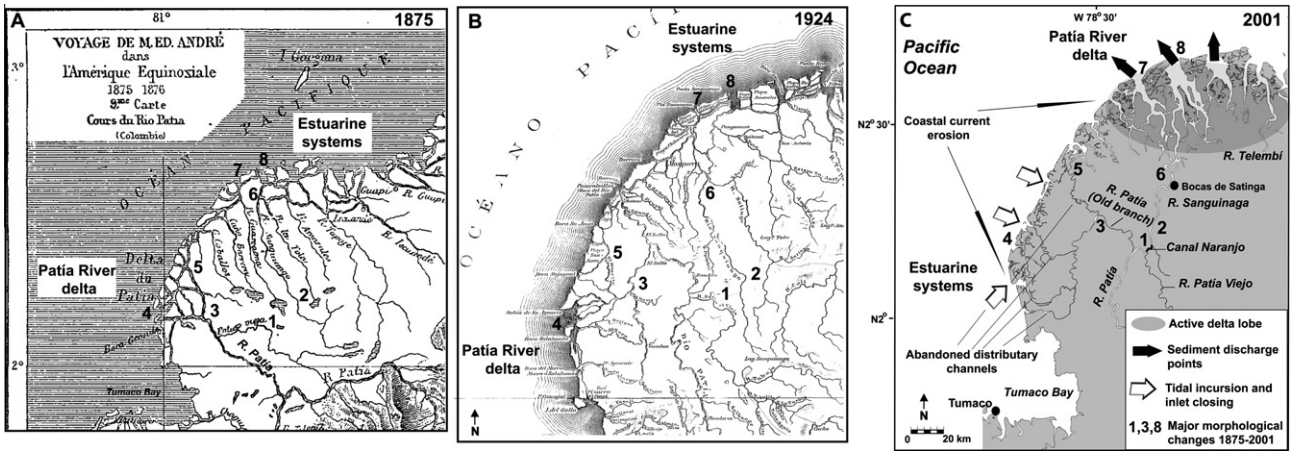

Fig. 6. Analysis of major morphological changes in the Patía delta from 1875 to 2001 based on a French Navy chart (1875) (A), a local map from 1924 (B), and a Landsat image from 2001 (C).

lobe, formation of ebb tidal deltas, and overall retreat conditions in the delta front; (5) coastline erosion at the former northern distributary, the Pasacaballos inlet; (6) active sedimentation at the new delta apex, Bocas de Satinga; and (7–8) migration of active fluvial discharge points from the southern delta lobe to the new active delta lobe. The barrier islands present in 1875 at Sanquianga and Amarales were accreted to the main delta lobe. Also, there is an evident widening of active distributary channels and overall frontal accretion of the Sanquianga River mouth (Fig. 6B and C).

4.4. Morphological changes during the 1962–2001 yr-period

Analysis of delta morphology in the southern delta lobe between 1962 and 2001 indicates major morphological changes during the 39-year period (Fig. 7), including: (1) strong retreating conditions at the San Juan barrier island; landward erosion resulted in a breaching event after the occurrence of the 1979 tsunami (Fig. 7A); (2) abandonment of active distributary channels as a result of the flow diversion from the Patía to the Sanquianga River; (3) closing of active distributary inlets at Majagual, Patía, and Salahonda (Fig. 7C–D); and (4) formation of ebb tidal deltas at the distributary mouths.

The southern Patía delta front, between Salahonda and Pasacaballos inlets (Fig. 1D), is experiencing shoreline retreating conditions. Table 1 summarizes the rates of shoreline change as averages of erosion values and percentages of transects in each coastal area experiencing erosion or accretion. Overall, 63% of the analyzed transects indicate retreating conditions. Higher erosion rates of 7.1 and 3.6 m yr^{-1} were observed at Pasacaballos and Patía inlets respectively, indicating coastal land losses of 106 m and 54 m for the 1986–2001 yr-period.

Along the northern delta front, erosion conditions are observed in 69% of the analyzed shoreline transects. Major retreating zones include Barrera, Guascama, Chitaco and Amarales barrier islands, with average coastal land losses of 153, 178, 136, and 131 m, respectively (Table 1). An erosional coastline with weak beach development, dead mangrove, and exposed peat soils in the surf zone characterizes the entire area.

The NWW3 wave data indicate that the observed waves in the Patía delta are predominantly swells from the southwest (77%) with a maximum monthly significant height of 2.2 m, and an average peak period of 14 s. Also, the AWAC time series measurements of wave parameters at five stations in the Patía delta front show that waves at the 10 m isobath have significant heights ranging from 0.54 to 1.4 m and a mean peak period of 14 ± 0.7 s. The analysis of total wave power per unit crest width along the delta front indicates that the Patía delta exhibits moderate wave energy conditions with an average wave power of $\sim 18 \times 10^6$ erg s^{-1} m at the 9 m depth contour.

4.5. Channel diversion and its environmental implications on the Patía River delta

4.5.1. Sedimentation within distributary channels and vegetation change

Fig. 8 shows major morphological changes that occurred in the current delta apex at Bocas de Satinga between 1962 and 2009. As a result of the channel diversion, the Sanquianga River is receiving most of the Patía sediment load. The migration of the active distributary channel from the southern lobe to the northern delta plain has led to active sedimentation, overbank flow, increasing width of levees, sedimentation in crevasses, interdistributary channel fill, and further lengthening of the Sanquianga River, the current main distributary channel.

We have inferred from the present mangrove distribution in the Sanquianga River several stages in the process of channel lengthening and the corresponding sequence of vegetation change (Fig. 9): (A) during the seaward advance of the Sanquianga distributary channel, submerged levees gradually emerge above sea level due to active sedimentation of fine sediment that deposited during overbank flow conditions; (B) pioneer mangroves start to colonize the fine sediments of levees and mudflats, particularly those areas which are exposed during low tide. Once the levee height above low water level reaches its maximum, the process of channel fill in the interdistributary channel begins; (C) after the interdistributary channel are filled, pioneer mangroves colonize the lateral channel; (D) the stages A, B, and C continue progressively downstream and the banks of the Sanquianga River show the sequence of longitudinal advance as seen by the periodic lows and highs of mangrove heights along the channel (Fig. 9, picture D).

We assume that this process of distributary channel advance was actively initiated after the diversion event started 37 years ago. According to local inhabitants, the colonization and further growth of these mangrove communities took place in approximately 30 years and sedimentation from the delta apex at Bocas de Satinga to the Sanquianga River became more pronounced since 1990s (Fig. 4). Although the conditions of channel diversion shifted the sedimentation from the Patía River to the Sanquianga, giving the constructive conditions for mangrove colonization, the increased water discharge has freshened the former estuarine

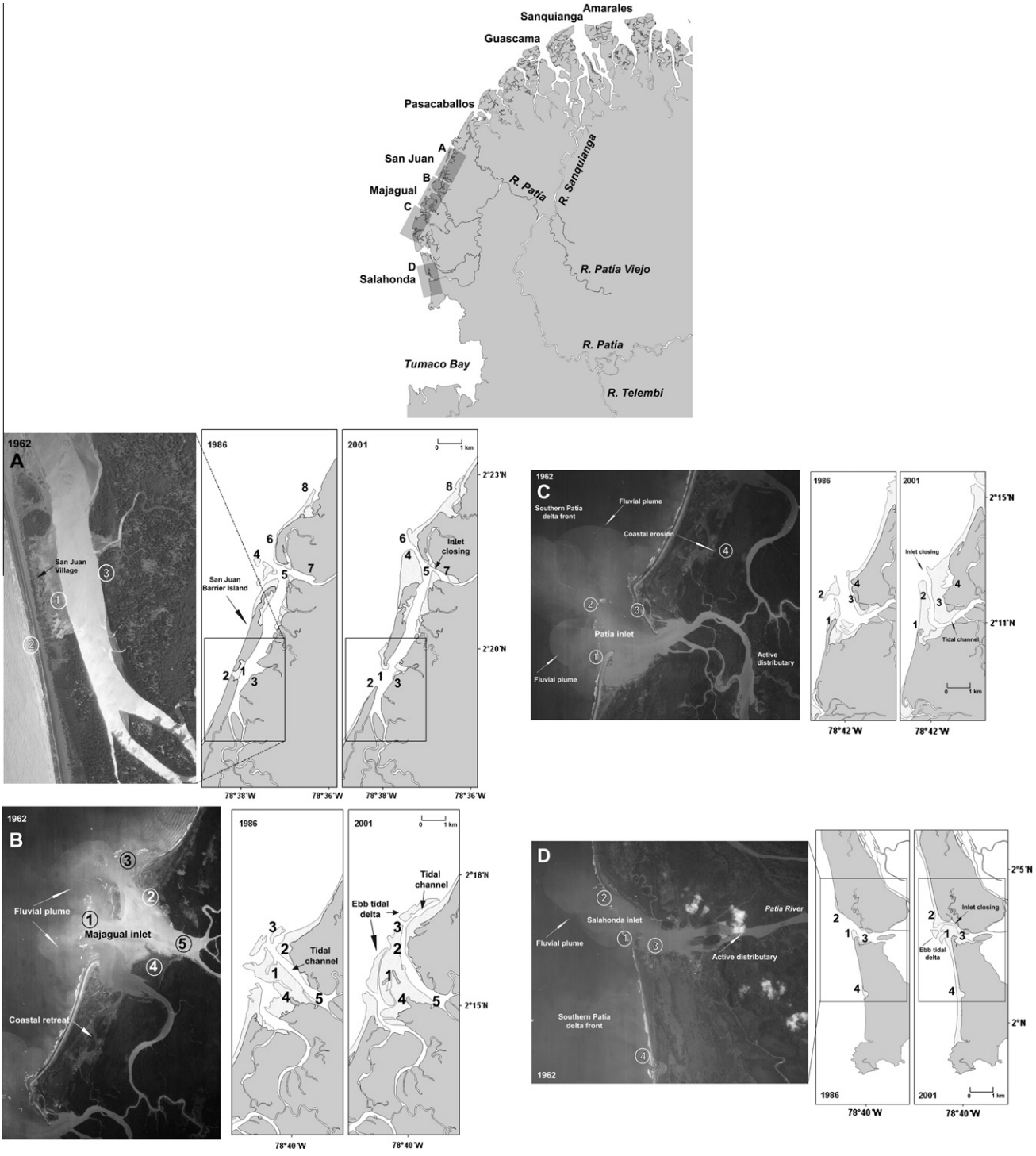

Fig. 7. Temporal analysis of morphological changes and channel closings along the southern delta coast based on aerial photographs from 1962 and Landsat images from 1986 and 2001. (A) San Juan barrier island, (B) Majagual inlet, (C) Patía inlet, and (D) Salahonda inlet.

system and created different hydrologic conditions with further ecological implications. This latter situation will be discussed later.

4.5.2. Relative sea-level and discharge diversion as major controls on mangrove erosion

The trend in relative sea level was estimated by least-squares linear regression for the Tumaco 1953–2006 time series (Figs. 1D and 10B). In Tumaco the relative sea-level rise measured $-0.6\ \mathrm{mm\ yr^{-1}}$ in the 1953–2006 period, indicating a decreased trend in sea level for the 53-year period. However, an increasing trend in relative sea level of $5.1\ \mathrm{mm\ yr^{-1}}$ is observed for the 1984–2006 period, after the occurrence of the 1979 tsunami (Fig. 10B).

At Tumaco (Fig. 1D), high sea level anomalies and the Southern Oscillation Index (SOI) show good coherence for the 53-year period 1953–2006 (Fig. 10C). Regression analysis between the smoothed sea level and the smoothed SOI yielded a coefficient of determination of $R^2 = 0.61$, a coefficient significant at the 95% confidence

Table 1
Coastline change trends in the Patía delta front derived from Landsat images 1986 and 2001 by using band ratio methods. The coastline rate of change was calculated by using DSAS software (Thieler et al., 2005) and two statistical estimates, including End Point Rate (EPR) and Linear Regression Rate of Change (WLR). The location of each coastline is shown in Fig. 8.

Coastline	Mean shoreline change (m yr^{-1})	Number of transects	Transects of erosion (%)	Transects of accretion (%)	Transects of no change (%)	Average distance of shoreline loss or accretion (m)
Southern delta lobe						
Salahonda	+1.09	73	16.4	80.8	2.7	+28.38
Hojasblancas	−1.25	67	64.2	31.3	4.4	−18.56
Patía	−3.60	101	72.3	22.8	4.9	−53.66
Majagual 2	−2.67	54	50.0	40.7	9.3	−39.75
Majagual 1	+4.51	10	10.0	90.0	0.0	+67.26
San Juan	+0.34	84	47.6	46.4	5.9	+5.04
Guandipa 2	−2.83	36	66.7	33.3	0.0	−42.17
Guandipa 1	+0.85	34	38.2	61.8	0.0	+12.65
Pasacaballos 2	−7.09	86	89.5	9.3	1.2	−105.82
Pasacaballos 1	−4.65	85	49.4	25.9	24.7	−37.56
Total southern delta lobe			63.2	31.7	5.1	
Northern delta lobe						
Paval 2	−5.08	23	73.9	26.1	0.0	−75.72
Paval 1	−5.17	11	100.0	0.0	0.0	−77.09
Barrera 2	−6.53	59	83.1	16.9	0.0	−97.44
Barrera 1	−10.23	31	90.3	9.7	0.0	−152.57
Chitaco 2	−1.71	11	100	0.0	0.0	−25.45
Chitaco 1	−11.97	33	75.8	21.2	3.0	−178.48
Guascama 4	−9.08	30	70.0	26.7	3.3	−135.59
Guascama 3	−5.41	22	77.3	22.7	0.0	−80.68
Guascama 2	−1.52	25	60.0	40.0	0.0	−22.69
Guascama 1	+3.41	6	16.7	83.3	0.0	+50.84
Sanguianga 2	−4.13	116	68.1	28.5	3.4	−61.54
Sanguianga 1	−1.74	52	59.6	28.8	11.5	−25.97
Amarales 3	+1.76	23	34.8	56.5	8.7	+26.27
Amarales 2	−8.78	41	63.4	12.2	24.4	−130.98
Amarales 1	−5.71	38	100	0.0	0.0	−85.22
Total northern delta lobe			69.1	22.6	8.3	

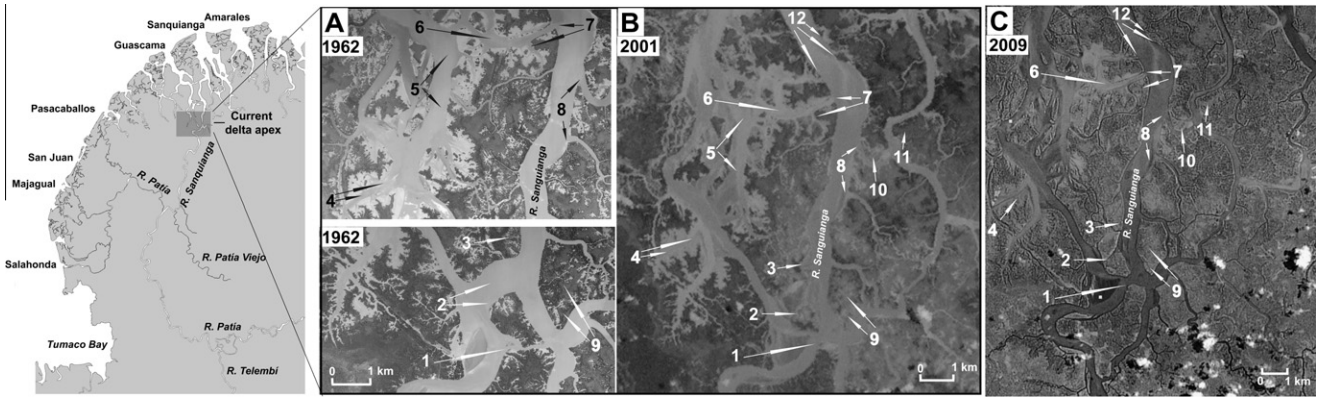

Fig. 8. Temporal analysis of morphological changes at the current delta apex, Bocas de Satinga, based on (A) aerial photographs from 1962 and (B and C) Landsat and Google images from 2001 and 2009, respectively. Numbers indicate major areas of sedimentation and channel fills in the Sanquianga distributary channel and associated tidal creeks.

level, which indicates that variations in the SOI explain 61% of the seasonal variability in water level, with low values of SOI corresponding to high Tumaco sea level anomalies. Hence, the sea level in the Patía delta is strongly affected by the Southern Oscillation.

Based on the NWW3 wave data 1978–2001, annual means of significant wave height (H_s) at the Patía delta front, are shown in Fig. 10D. Overall, there is a good agreement between sea-level anomalies during El Niño events and significant wave heights. During El Niño periods in 1982–1983, 1987–1988, 1992–1993, and 1997–1998, H_s were considerably higher than the interannual mean of 0.93 m. In general, wave heights during raised sea-level conditions are higher than the interannual mean by 30%, indicating increasing wave energy conditions at the Patía delta coast.

As a result of relative sea-level rise (Fig. 10B), transgressive barrier islands are present along the northern Patía delta front (Figs. 7 and 11). These islands appear to migrate because the front side of the island is constantly eroded by wave action. These islands lack healthy dune systems and backshore vegetation that act as sand anchors on the beach. This deficiency makes the island susceptible to erosion, allowing wind-generated waves to carry sediment from the beaches to the backside of the island. Due to the flooding of storm waves over the island, dead mangroves of *Rhizophora* and

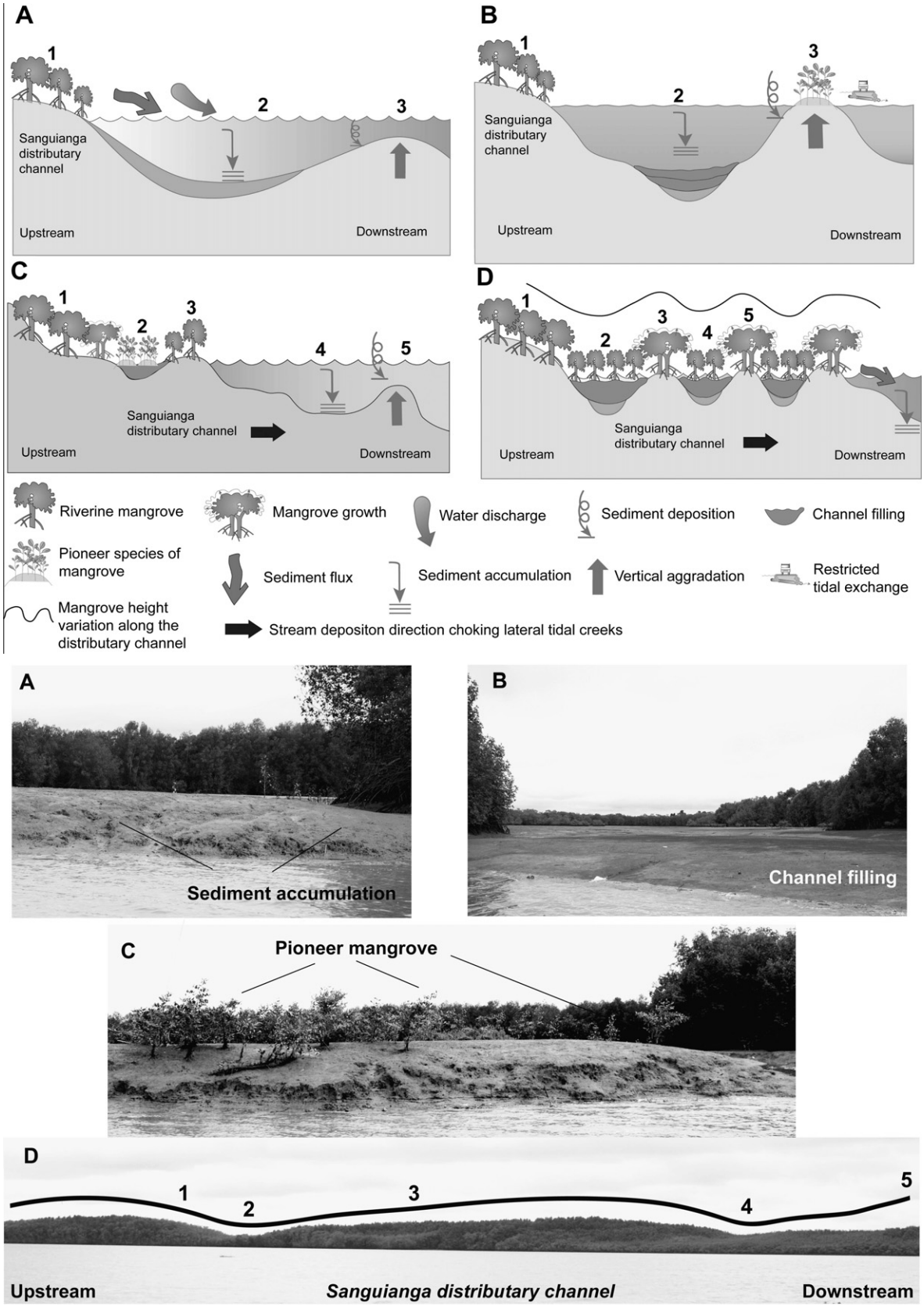

Fig. 9. (A–D) Stages of channel lengthening and corresponding sequences of mangrove colonization along the Sanquianga distributary channel.

Avicennia as well as peat soils of former backside mangrove swamps are exposed on the shoreline (Fig. 11).

Ongoing subsidence of the entire delta plain is an important factor in the fluvial sediment supply to the islands. Channel switching

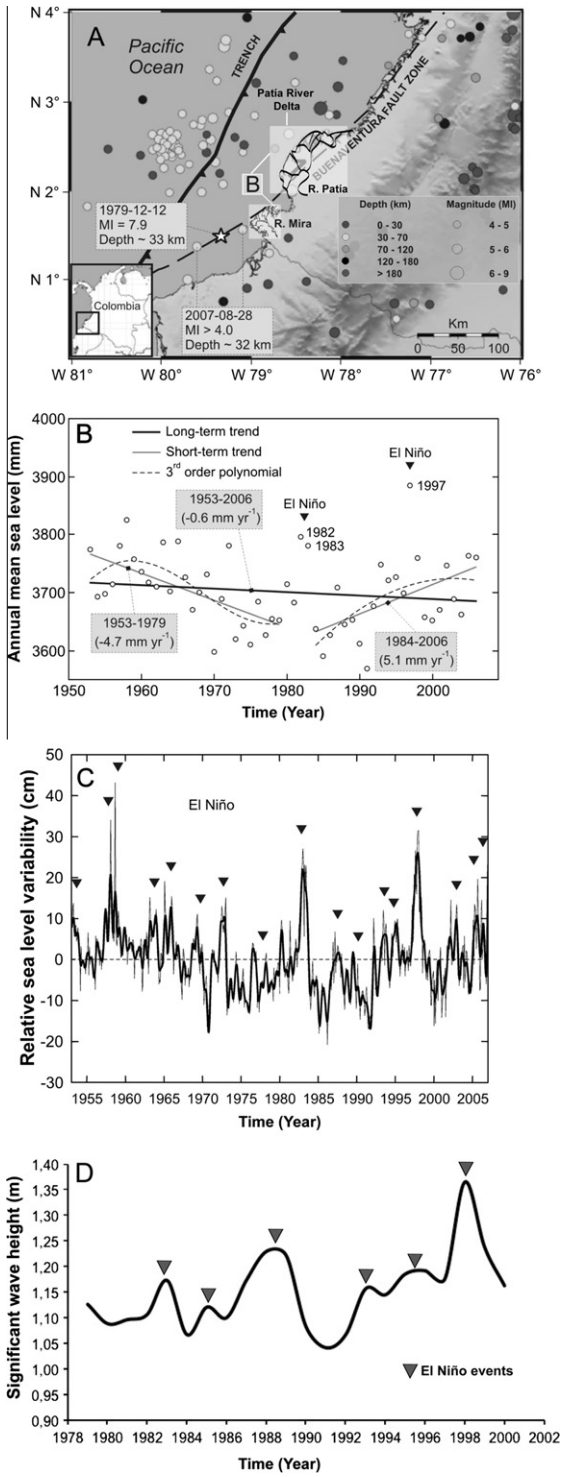

Fig. 10. (A) Location and magnitude of earthquakes that occurred in the southern Colombian Pacific between 1993 and 2007. More than 120 seismic events with magnitudes (MI) greater than 4, were recorded by the Geological Survey of Colombia between 1993 and 2007 (INGEOMINAS, 2007). Also shown are the locations of two recent seismic events (August 2007) and the tsunami (December 1979) (white star) that impacted the Patía delta coast. (B) Mean relative sea-level (mm) from Tumaco, Pacific coast of Colombia (IDEAM, 2007), showing the trend for the 1953–2006 period with slope = −0.6 mm yr^{-1} (bold line) and the short-term trends (gray line) for the 1953–1979 period (slope = −4.7 mm yr^{-1}) and 1984–2006 period (slope = 5.1 mm yr^{-1}). Solid triangles indicate the occurrence of two major El Niño sea-level anomalies in 1982–1983 and 1997, which were removed from the analysis (modified from López et al., 2009). (C) Monthly average (thin line) and low-frequency pass filter with zero-phase (bold line) plots of water-level anomalies at Tumaco in 1953–2006. (D) Plot of annual means of significant wave height (H_s) at the Patía delta front derived from the NWW3 wave data 1978–2001.

deprives the delta of sediment as the abandoned areas subside, the older distributary mouths become flooded or drowned. This may be the former case of the northern Patía River delta before the channel diversion occurred. In contrast, current conditions are characterized by active sedimentation at the delta apex, downstream channel accretion and sediment deposition in estuarine lagoons (Fig. 8). Although the northern delta lobe shows signs of coastal subsidence along transgressive barrier islands (Figs. 7 and 11), our analysis of satellite images during low tide conditions for the 1986–2001 yr-period in the Sanquianga inlet, indicates an increase in tidal flat area from 5.4 M m^2 in 1986 to 14 M m^2 in 2001. Hence, the Sanquianga River, a distributary channel experiencing an accretional phase, is switching from previous estuarine conditions to an active delta system.

The so called erosion of mangroves is also a common geomorphic feature in the Patía southern delta lobe. This former delta plain, exposed to predominant wind waves from the southwest, lacks sufficient sediment for the offshore zone to build shoals, which could mitigate the effects of wave action and sea level rise. Some barrier islands, including those at Pasacaballos and San Juan de la Costa (Fig. 7), experienced higher rates of erosion after the occurrence of the 1979 tsunami and the more pronounced flow diversion during the 1980s (Fig. 4). The sand starving conditions, associated with channel abandonment and river mouth switching to the north, may account for narrower islands and steeper subaqueous profiles of shallow coastal platforms.

4.5.3. Changes in longitudinal salinity distribution and their impact on mangroves

Along the former active distributary channels on the southern delta lobe, maximum mangrove intrusion is ~6 km upstream (Fig. 6), and vegetation succession from freshwater to brackish conditions is characterized by: (1) association of freshwater forests; (2) a brackish zone where salinity varies between 4 and 8 psu, the mangrove *Mora oleifera* is associated with palms and trees typical of freshwater swamps; and (3) near the mouths, red mangrove communities of *Rhizophora* occupying channel banks and black mangrove *Avicennia* are more dominant in the higher and drier habitats.

The northern delta lobe, the Sanquianga area, an estuarine zone characterized by the presence of well-developed belts of *Rhizophora* and *Avicennia* along the edge of the estuarine lagoons and tidal channels, became an active distributary system after the channel diversion of the Patía River. Longitudinal measurements of vertical profiles of salinity (psu) along the main axis of distributary channels, including Sanquianga, Guascama and Amarales (Fig. 12A), show clear dependence on the discharge pattern of the deltaic plain. Prior the channel diversion, the 1 salinity interface at the bottom intruded 27 km further upstream up to Bocas de Satinga, the current delta apex. Nowadays the 0 salinity interface near the bottom was found 12, 14 and 24 km upstream on the Sanquianga, Guascama, and Amarales distributaries, respectively. The longitudinal salinity distribution qualitatively reflects the amount of freshwater discharged by the Sanguinga River. Also, the effect of increased freshwater after the channel diversion is to flush out the wedges of saline waters from the main distributary channels. In contrast, abandoned distributaries of the former Patía delta, which currently lack fluvial flows for at least 8 months each year, posses more saline waters and exhibit salinity distributions further upstream.

Freshening conditions in the Sanquianga distributary channel have shifted the upper estuarine region downstream (salinity <1) (Fig. 12A). According to natural experts in the area (from personal communication with Wilfrido Ibarbo), the effect of increased freshwater discharge on plant ecology has become more pronounced during the last decade. Near the current delta apex at Bocas de

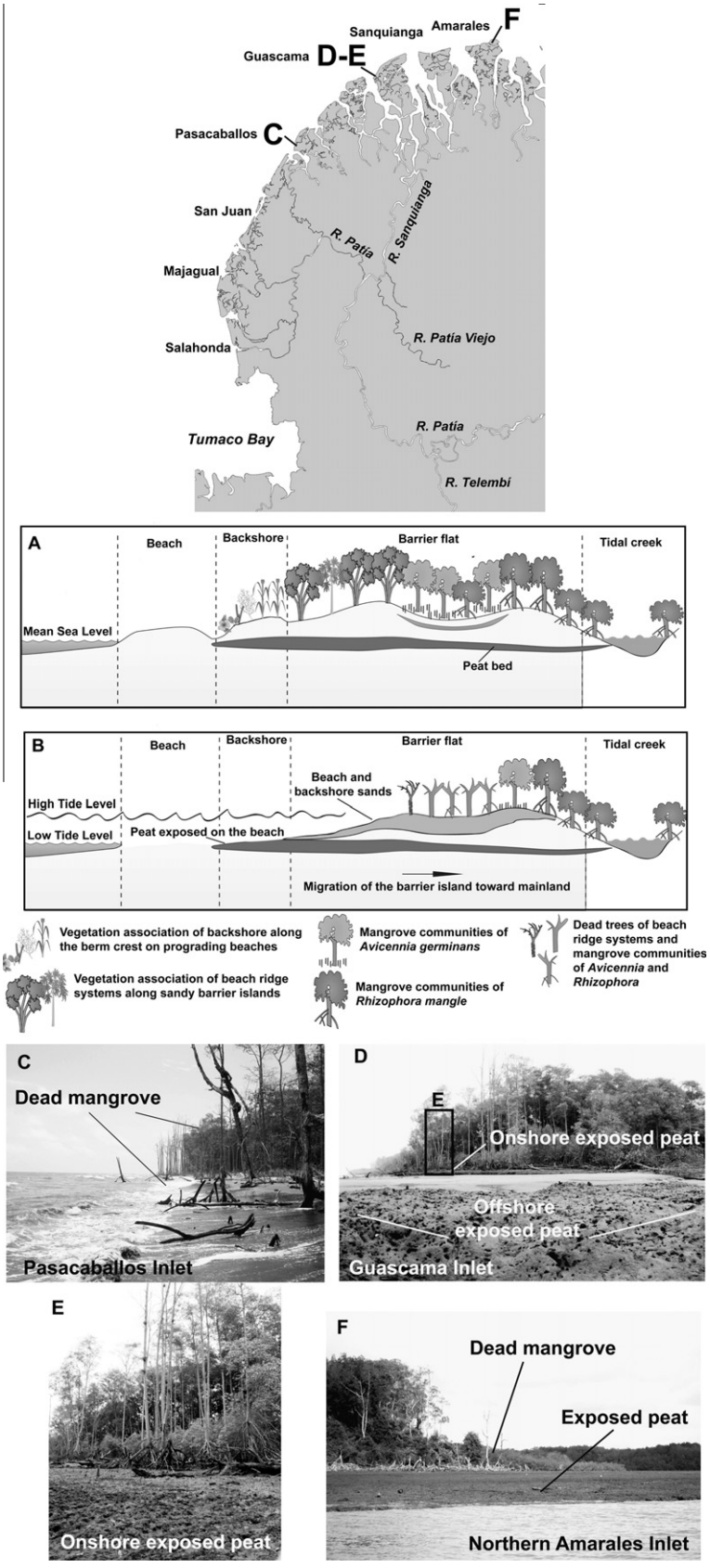

Fig. 11. (A) Scheme of a transgressive barrier island along the southern lobe of the Patía delta. (B) Transgressive barrier islands migrate landward and peat soils become exposed on the oceanfront, due to tectonic induced subsidence and sediment starving conditions after the channel diversion in 1972. We also show exposed peat soils on the beach along barrier islands in the southern (C–E) and northern (F) delta fronts. Note strong conditions of mangrove erosion on the shoreline.

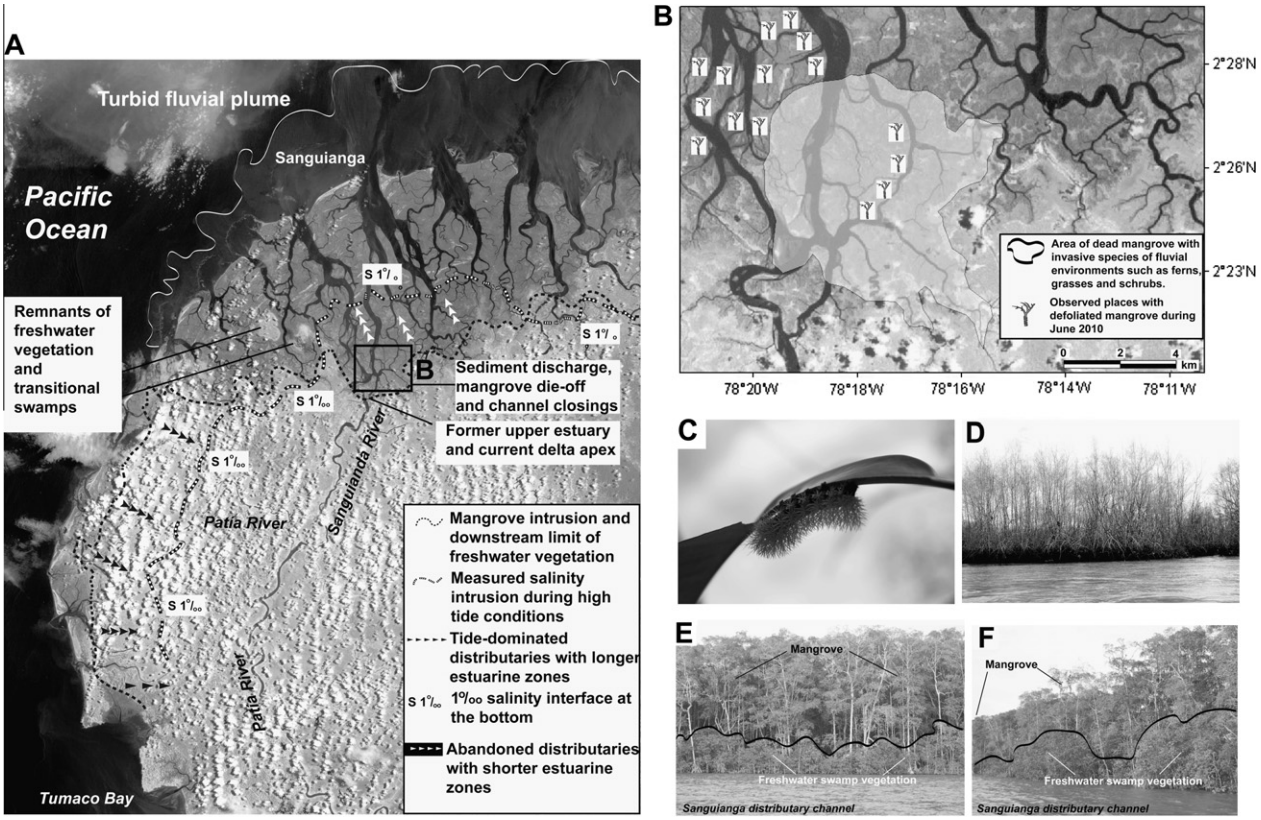

Fig. 12. (A) Aster image from 2008, showing major longitudinal limits of salinity intrusion and downstream limits of freshwater vegetation. (B) Landsat image from 2001, showing the area of mangrove die-off near Bocas de Satinga, where highest sediment accumulation rates occur. Also, areas of defoliated mangrove observed during the field sampling in June 2003, are shown. (C and D) Defoliated mangrove communities of *Rhizophora* and *Avicennia.* Under environmental stressors (e.g., changing conditions of salinity and sediment deposition), mangrove forests become more vulnerable to warm plagues like the one observed in Sanguanga (Saturnidae family) (C). (E and F) Mangroves of *Mora oleifera*, a mangrove tolerant of brackish water, and also characteristic of the freshwater swamp zone, are invading channel banks in the lower and mixing estuarine zone.

Satinga, characteristic grasses of fluvial environments such as *Panicum* and *Paspalum,* are colonizing point bars and mud flats in front of the channel banks with are vegetated by *Rhizophora*. In addition, hugo trees, locally called Nato (*Mora oleifera*), a mangrove tolerant of brackish water and also characteristic for the freshwater swamp zone, are invading channel banks in the lower and mixing estuarine zones (Fig. 12E and F). Further environmental consequences include the die-off of approximately 5200 ha of mangrove near Bocas de Satinga, where highest sediment accumulation rates occur (Fig. 12B). These zones have been colonized by the opportunistic fern *Acrostrichium aureum* and other shrubs characteristic of freshwater environments.

Another environmental issue observed in the Sanquianga Mangrove National Park (SMNP) has been the recurrent periods of mangrove defoliation (Fig. 12D), which, prior the channel diversion, were not seen in the area. Under environmental stressors, mangrove communities become more vulnerable to plagues like the one present in the SMNP, a larval of the *Saturnidae* family (Fig. 12C).

5. Discussion

Climate determines where tropical weathering occurs, while tectonics increase erosion rates and dictates the composition of erosion products (Stallard, 1988). Drainage basins with intense tectonic activity, like those located on active margins, usually have high sediment yields (Meade, 1988; Milliman and Syvitski, 1992), as in the case of Colombian Pacific Rivers (Restrepo and Kjerfve, 2000). Besides climate and weathering factors, other processes such as landslides lead to slumps that increase sediment loads. In humid uplands, landslides are the dominant mass wasting process (Hovius, 1998). The Patía drainage basin is characterized by the presence of active fault systems, high precipitation rates, slopes frequently steeper than 25° (Fig. 2B), and dense tropical rain forests. According to Hovius et al. (1997), these conditions are favorable to the occurrence of rapid mass wasting caused mainly by hillslope erosion processes such as landslides and slumps.

In addition to natural forces controlling sediment load of rivers, human activity can also be an effective geologic agent in altering the landscape, influencing sediment fluxes in the river. Although the anthropogenic impact on global fluvial sediment fluxes cannot yet be calculated to a high degree of accuracy, human activity may be directly or indirectly responsible for 80% to 90% of the fluvial sediment delivery to the coastal ocean in regions unaffected by trapping of sediment by reservoirs (Farnsworth and Milliman, 2003). In contrast to decreased erosion rates and therefore decreased sediment transport by rivers in much of the developed western world, erosion is increasing throughout many developing countries (Syvitski, 2003). In this, Colombia is not an exception (Restrepo and Syvitski, 2006). For the Patía drainage basin, many human-induced drivers, including deforestation, land conversion due to agricultural and mining practices, may have accounted for the overall increasing trends in specific sediment yield.

As mentioned before, the main distributary channel of the Patía River shifted to the south in the Holocene, probably as a result of tectonic activity. There are a wide variety of barrier island shapes and sizes related to island position with respect to active distributaries, and constructional versus destructional segments of the

Patía delta plain. Martínez et al. (1995) analyzed the evolution of barrier islands along the Pacific coast of Colombia, including the islands of the Patía River delta. In their study, which analyzes major morphological changes between 1962 and 1986, they recognized strong erosion conditions in the northern islands of the delta, reflecting both rapid subsidence and insufficient sand supply to maintain inlet cross-sections in equilibrium with the tidal prism. In contrast, the authors observed that in the southern active delta edge, islands are fronted by beaches and are more substantial in area. According to this study, the larger sand supply for this southern delta segment contributes to larger islands and active dune formation. Only two shoreline areas, Hojas Blancas and Salahonda, showed signs of erosion (Martínez et al., 1995). When comparing our analysis of shoreline changes (Table 1) with the one previously discussed (Martínez et al., 1995), it may be possible that erosion conditions in the southern delta front increased after 1987, when the discharge diversion to the north of the Patía River became more pronounced (Fig. 4).

The degree to which wave power is reduced by the offshore slope is indexed by an attenuation ratio (A_p). This index, developed by Bretschneider (1954) and Bretschneider and Reid (1954), estimates the reduction of wave height due to bottom friction (Wright and Coleman, 1971). In the Patía delta, the attenuation ratios indicate that friction reduces nearshore power to 16% in the Pasacaballos inlet of the deep-water power, while in the Guascama and Sanquianga inlets, the A_p values are higher and wave power is reduced by 67% and 82%, respectively. The steeper profile in the southern delta plain at Pasacaballos causes low reduction of wave power due to friction. This morphologic condition may be responsible for the lowest attenuation ratio along the Patía delta front, and hence, stronger erosional conditions at Pascaballos compared to the lower values of coastal retreat in Guascama and Sanquianga inlets (Table 1).

Along the Patía delta front, more than 20 earthquakes with magnitude 4–6 occurred within 200 km of the shoreline from 1993 to 2007 (López et al., 2009) (Fig. 10A). In addition, most intense earthquakes during the 20th century occurred in 1906 and 1979, and caused both regional and local subsidence. During the tsunami in 1979, coastal areas of the Patía delta, including San Juan de la Costa and the northern distributaries at Sanquianga (Fig. 1D), subsided as much as 1.6 m, causing an apparent sea level rise along at least a 200 km stretch of the Colombian coast north of the Ecuadorian border (Herd et al., 1992).

It is well documented that when relative sea level increases, deltaic lowlands become more vulnerable to inundation, flood events and erosion (e.g. Day et al., 1995; Ericson et al., 2006). In the Pacific deltas of Colombia there are no quantitative measurements of recent coastal subsidence to verify tectonic subsidence. However, few qualitative evidences in the Pacific deltas suggest that subsidence is occurring in this part of the coast (Restrepo et al., 2002), including (1) the correspondence of increasing trend in relative sea level with tectonic setting (Fig. 10B), (2) the increased occurrence of non-storm washover events and earthquake activity, and (3) transgressive barrier islands with exposed peat soils on the beach front (Fig. 11).

The mentioned changes observed in the mangroves of the SMNP are primarily the response to an ever-changing series of habitats, the result of geomorphic changes associated with the development of an active delta plain. Similar processes have been observed in other deltas, including Tabasco, Mexico (Thom, 1967), Mira and San Juan, on the Pacific coast (Restrepo et al., 2002), Atrato, on the Caribbean coast of Colombia (Vann, 1959), and are similar to the Purari, Papua New Guinea (Conn, 1983).

It is worth mentioning that the current active distributary channel, the Sanquianga, was an estuarine system with very low inputs of freshwater discharge and sediment load. These hydrologic conditions, together with the mesotidal range, characterize this part of the coast, favoring the formation of extensive mangrove swamps. According to Thom (1967), mangroves are not present unless the stream is in deteriorating phase, otherwise, freshwater plants would occupy this habitat. Also, mangroves on natural levees simply indicate channel deterioration and hence the presence of saline water at any given time. Thus the observed ecological changes in the northern lobe of the Patía delta are the first environmental signs of shifting conditions from an estuary to a delta system as these processes act on long-term time scales.

6. Further environmental implications

6.1. Discharge diversion and its impact on coral reef ecosystems of Gorgona Island

The Gorgona Island, the largest and best-developed coral reef complex of the eastern tropical Pacific, that constitutes a marine protected area, is located 29 km offshore from the Sanquianga inlet (Figs. 1D and 13). Scientists and decision-makers in Colombia are not aware whether and to what extent the fluxes from the Sanquianga River, after the discharge diversion occurred, impact the coral reefs ecosystems of Gorgona Island.

Examining images from the Moderate Resolution Imaging Spectroradiometer (MODIS) satellite (Fig. 13), the Sanquianga River enters the Pacific coast as a low-salinity river plume deflected westward from the Sanquianga inlet and northward from the entrance at Amarales. Seaward advection is more pronounced during November, a period that coincides with the highest seasonal water and sediment discharges. It is worth noting that fluvial plumes in November appear to shift offshore to Gorgona Island. Further analysis of Landsat and MODIS images between 2000 and 2008 (all images coinciding with low tide conditions), indicate that these plume fronts are not present along the southern delta coast. Turbidity waters rather correspond to re-suspension of coastal sediments due to wave shoaling processes.

Vertical CTD profiles along longitudinal transects 20–25 km seaward of the Sanquianga and Amarales mouths during November 2010 (Figs. 1D and 13A), a period of anomalous high discharge due to La Niña event, indicate surface salinities of 22 psu in Gorgona Island. The near-surface layer in the Sanquianga–Gorgona transect is separated from the underlying water masses by a sharp halocline of approximately 2 m thickness (Fig. 13G). These plume fronts were clearly visible during the field sampling as straight lines separating brown fluvial water from the surrounding seawater. The low turbidity seaward of these fronts indicates that most sediment has already settled from suspension. Also, the vertical distribution of salinity in the Amarales–Gorgona transect (Fig. 13H), with a halocline of 7 m thickness and surface salinities of 28 psu, indicates a northwest shift of the river plume from the Sanquianga and Amarales entrances. In contrast, surface salinities of 29 and 30 psu, measured in front of the Pasacaballos and Salahonda mouths, respectively (Fig. 13I and J), indicate less fluvial effect along the abandoned delta coast. Even higher surface salinities (31 psu) are observed just 5 km offshore from these inlets.

We are not aware of previous vertical profiles of salinity along longitudinal transects between the Sanquianga inlet and Gorgona Island. In addition, surface salinities as low as 22 psu have not been documented before. During an oceanographic survey in September 2006, Giraldo et al. (2008) measured surface salinities of 25 psu in Gorgona Island, but the authors did not follow the turbid plume from the Sanquianga or Amarales entrances. The brackish character of ocean waters observed in Gorgona clearly reflects that the Sanquianga fluvial plume is affecting water quality and reducing salinity. Although live coral cover remains high, the immediate future of the Gorgona reefs gives cause for concern. Similar to other

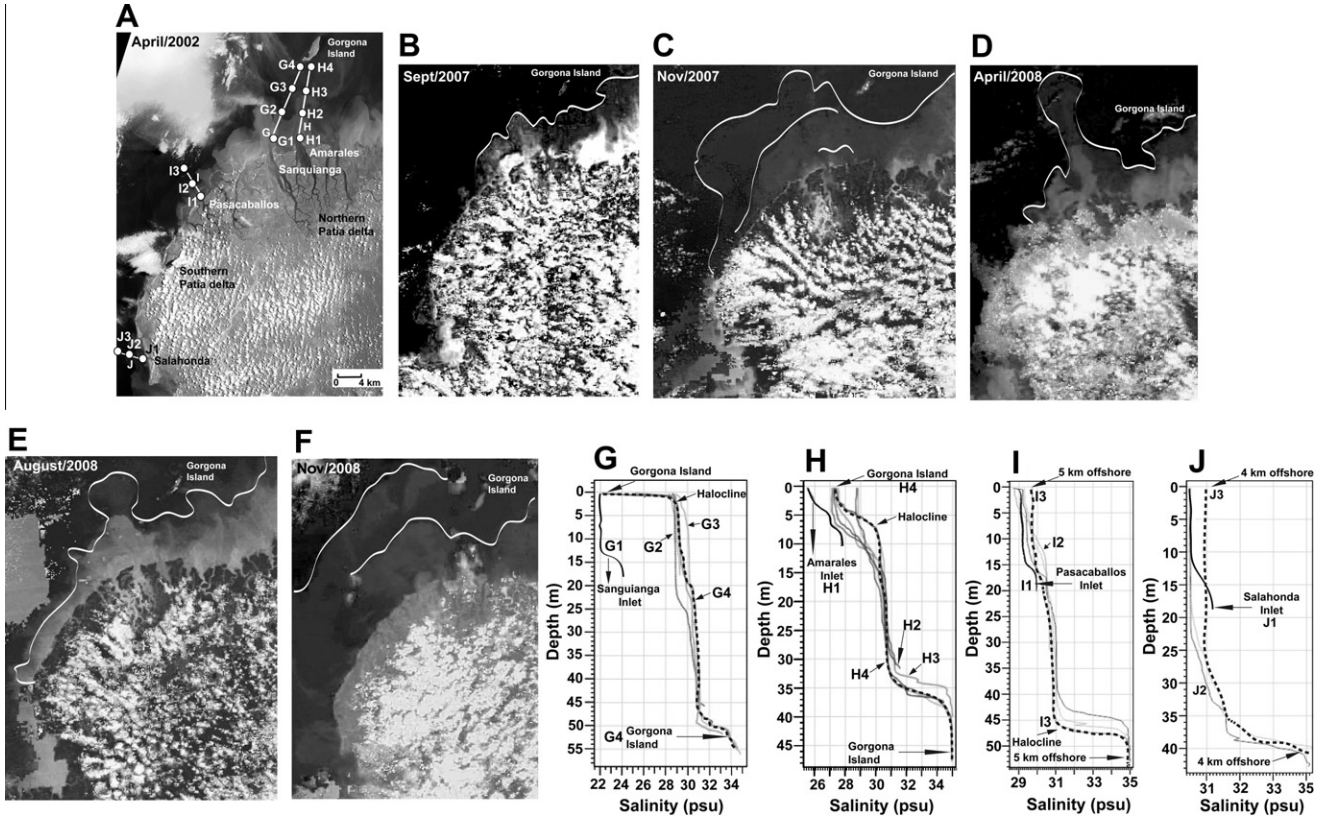

Fig. 13. Fluvial plume of the Sanquianga River viewed from Landsat (A) and (B–F) MODIS satellite images. White lines follow the turbidity plume dispersal. Locations of the CTD profiles at delta front sites are also shown. We also indicate the location of Gorgona Island where the coral reef complex is located. (G–J) Vertical salinity profiles at each CTD transect along the delta front, including Sanquianga (G), Amarales (H), Pasacaballos (I), and Salahonda (J). These CTD transects were sampled during November 2010.

coral reefs worldwide, there has been a mix of multiple stressors (natural and anthropogenic; local, regional and global; temporal and chronic) affecting coral reefs. In order to provide direct evidence of impacts of sedimentation from the Saquianga River, national coastal surveys should measure and analyze water-quality parameters in places of the Gorgona Island.

6.2. Deforestation within the Patía drainage basin and associated impacts on the Sanquianga Mangrove National Park

Recent deforestation estimates in the Andes of Colombia have shown that the percentage of forest cover in e.g. the Magdalena basin, the largest Andean basin in South America, has declined from 46% in 1970 to 27% in 1990, with an annual deforestation rate of 1.9%, or 234 000 ha yr^{-1} (Restrepo and Syvitski, 2006). For the whole country, IDEAM estimated an overall annual deforestation of 336,000 ha yr^{-1} between 2000 and 2009. This loss in forested area in Colombia is considered to be among the highest in the world, representing deforestation trends that are also observed in the Brazilian Amazon and Indonesia (FAO, 2009).

During the 1970s, the Colombian government gave many licenses to big logging companies such as Cartón de Colombia and Maderas Pizano, among others, to clear cut forests in the Patía drainage basin and its delta. According to the National Department of Statistics (Dane, 2003), 60% of the wood production in the country came from the Patía region. Many sawmills went out of business later in the eighties, since most of commercial forests in the catchment were removed. In Bocas de Satinga, along the Sanguianga River (Fig. 1D), there were more than 40 sawmills during the seventies. Nowadays only two sawmills remain. After harvesting most of the wood resources, an economic down was evident in the region.

The illicit drug trade of coca in Colombia, Peru and Bolivia has been identified as a contributor to deforestation in the tropical Andes (Harden, 2006). The US Department OF State (2001) estimated that a minimum of 2.4 Mha of forest were cleared for coca production in the Andean region over the previous 20 years. The environmental report of Colombia, a study made by the World Bank (Sánchez-Triana et al., 2007), estimated that at least 850,000 ha of forest were also cleared for coca production in the Colombian Andes between 1978 and 1998. A recent survey in the Pacific forests, including the Patía River drainage basin, has shown a dramatic expansion of the area of deforestation due to cocaine crops. Alone in the Patía River catchment, including a major tributary system, the Telembí River (Fig. 2A), approximately 12,000 ha of forest were cleared for cocaine crops since mid 1990s. This is the largest area of cocaine cultivation in the country (UNODC, 2009).

Clearance of natural vegetation for land cultivation is known to cause increased rates of soil erosion (Walling and Fang, 2003). Increases in soil erosion rates may range several orders of magnitude over various areas of the world development (Morgan, 1986). The significance of this land use impact on soil erosion rates is emphasized by a global survey of soil degradation, which indicated that nearly 10% of the world's land surface is currently affected by water erosion (Oldeman et al., 1991). In the Andes of Colombia, such increases in soil erosion rates are likely to be reflected in increased river sediment loads (Restrepo and Syvitski, 2006). The results presented in this paper show that the Patía River has experienced significant increases in sediment yield over the 1970–1980 and 1990–2000 decades (Fig. 3), both time periods corresponding with sustained land degradation due to deforestation.

The Patía River appears to have the highest sediment yield of the medium-large rivers along the Atlantic and Pacific coasts of South

America. Its yield, 1500 t km^{-2} yr^{-1}, is higher than the previous top one value reported for the San Juan River on the Pacific Colombia, 1150 t km^{-2} yr^{-1} (Restrepo and Kjerfve, 2000), almost four times greater than the yield of the Amazon, 167 t km^{-2} yr^{-1}, Orinoco, 158 t km^{-2} yr^{-1} (Latrubesse et al., 2005), or Negro (Argentina), 140 t km^{-2} yr^{-1} (Milliman and Syvitski, 1992), and much greater than the yield of the Paraná, 43 t km^{-2} yr^{-1}, Uruguay, 164 t km^{-2} yr^{-1} (Latrubesse et al., 2005), and São Francisco, 10 t km^{-2} yr^{-1} (Milliman and Syvitski, 1992). Our conclusion is that many natural and human induced controls, including (1) high run-off conditions, (2) steep relief within catchment, (3) low discharge variability, (4) episodic sediment delivery due to either geologic events or climatic anomalies, and (5) ongoing land degradation due to deforestation, may account for this high sediment yield.

7. Conclusions

The results presented here show that a former estuarine system, with the largest mangrove reserve in Colombia, located on the west coast of South America, is becoming an active delta system with the highest sediment yield of any documented Andean River. Under these environmental conditions, we expect that the ecological changes in the mangrove communities of the SMNP will be enhanced as a result of ongoing trends of deforestation, soil erosion, and increasing sediment load in the upper catchment.

As mentioned before, the high sediment and freshwater inputs into the mangrove ecosystem create additional stress (both at ongoing background levels and, occasionally, at dramatic levels), which may periodically push local environmental parameters beyond the thresholds for mangrove survival. The Patía River deserves international attention. It is the largest fluvial system discharging directly into the western coast of South America. Thus, the synthesis and preliminary analysis presented in this paper are the first step toward understanding the natural and anthropogenic factors that have produced the observed patterns of delta shift of the Patía River, and to relating these processes to the impact on the natural aspects of delta ecosystems.

The preliminary results allow us to formulate a hypothesis that, with increasing human activities on the Patía catchment, the affected area is significant and will continue to increase in both size and degree of how it is affected unless human influences are curtailed. Further studies should develop models to enable quantification of the effect of various scenarios for control of land-use activities anywhere. These investigations should also offer decision-makers and the public a science-based tool to decide what activities should be allowed, and how they should be controlled, in the drainage basins and at delta coast, in order to produce a desired state of health for mangroves, coral reefs, other coastal ecosystems and for the people who live on the Patía delta. The future state of health for the Sanguianga Mangrove National Reserve deserves more scientific and governmental attention.

Acknowledgments

This study is supported by the Instituto Nacional para el Desarrollo de la Ciencia y la Tecnología "Francisco José de Caldas", COLCIENCIAS, grant 1216-452-21267 (Morphodynamics of the Patía River delta, Pacific coast of Colombia), EAFIT University – Department of Geological Sciences-, and the Colombian Port Authority, DIMAR, through its research institute CCCP (Centro de Investigaciones Oceanográficas del Pacífico) in Tumaco, Colombia. Special thanks to the crew of the ARC Gorgona and its captain German Rojas, for their support and friendship during the oceanographic cruises. Further support is provided by the National Science Foundation of the United States of America, Award Number: 0952116. Also, we are very grateful to the native experts of the Sanquianga Mangrove National Park, specially Wilfrido Ibarbo, for their support during the sampling trips in the area.

References

Arango, J.L., Ponce, A., 1982. Mapa geológico del Departamento de Nariño, Escala 1: 400,000, Memoria Explicativa. Ingeominas, Bogotá, p. 88.
Ashton, A., Murray, A.B., Arnoult, O., 2001. Formation of coastline features by large-scale instabilities induced by high-angle waves. Nature 414, 296–300.
Bateman, A., Medina, V., Coliles, A., Loaiza, A., García, W., Puig, C., 2009. The impressive case of the uncontrolled diversion of the Patía River at its delta and the social and environmental consequences. In: Proceedings of the Congress of River, Coastal and Estuarine Morphodynamics (RCEM, 2009). Universidad Nacional del Litoral, Santa Fe, Argentina.
Berry, P.A.M., Garlick, J.D., Smith, R.G., 2007. Near-global validation of the SRTM DEM using satellite radar altimetry. Remote Sens. Environ. 106, 17–27.
Bretschneider, C.L., 1954. Field Investigation of Wave Energy Loss in Shallow Water Ocean Waves. US Army Corps Engineers Beach Erosion Board Tech. Special Publication 46, pp. 1–21.
Bretschneider, C.L., Reid, O., 1954. Modification of Wave Height due to Bottom Friction, Percolation and Refraction. US Army Corps Engineers Beach Erosion Board Tech. Special Publication 45, p. 36.
Buchanan, T.J., Somers, W.P., 1969. Discharge Measurements at Gauging Stations. Techniques of Water Resources Investigations of the US Geological Survey (Book 3, chap. A8). Government Printing Office, Washington, DC.
Case, J.E., Durán, L.E., López, A., Moore, W.R., 1971. Tectonic investigations in western Colombia and eastern Panamá. Geol. Soc. Am. Bull. 82, 2685–2712.
Cediel, F., Shawn J., Caceres, C., 2003. Tectonic assembly of the northern andean block. In: Bartolini, C., Buffler, R., Blickwede, J., (Eds.), The Gulf of Mexico and Caribbean Region: Hydrocarbon Habitats, Basin Formation and Plate Tectonics, AAPG Memoir 79. AAPG, Tulsa, OK, pp. 815–848.
Conn, B.J., 1983. Aquatic and semi-aquatic flora of the Purari River system. In: Petr, T. (Ed.), The Purari-Tropical Environment of a High Rainfall River Basin. Dr. W. Junk Publishers. The Hague, The Netherlands, pp. 283–293.
Correa, I.D., 1996. Le littoral Pacifique Colombien: interdependance des agents morphostructuraux et hydrodynamiques - Tome 1: texte. Ph.D. dissertation, Universite Bordeaux I, Bordeaux, France, 178.
Correa, I.D., González, J.L.,1988. Geomorfología general y sedimentología de la Bahía de Tumaco. INGEOMINAS-CCCP-PROGOG, Tumaco. 58.
Dane, 2003. Departamento Administrativo Nacional de Estadística. Statistical Information. <http://www.dane.gov.co/inf_est.htm.2003>.
Day, J.W., Giosan, L., 2008. Geomorphology: survive or subside? Nat. Geosci. 1, 156–157.
Day, J.W., Pont, D., Hensel, P.F., Ibañez, C., 1995. Impacts of sea-level rise on deltas in the Gulf of Mexico and the Mediterranean: the importance of pulsing events to sustainability. Estuaries 18, 636–647.
Enfield, D.B., Allen, J.S., 1980. On the structure and dynamics of monthly mean sea levels anomalies along the Pacific coast of North and South America. J. Phys. Oceanogr. 10, 557–578.
Ericson, J.P., Vörösmarty, C.J., Dingman, S.L., Ward, L.G., Meybeck, M., 2006. Effective sea-level rise and deltas: causes of change and human dimension implications. Global Planet Change 50, 63–82.
Etayo-Serna, F. (Ed.), 1983. Mapa de Terrenos Geológicos de Colombia. Publicaciones Geológicas Especiales del INGEOMINAS. INGEOMINAS, Bogotá. 235.
FAO, 2009. State of the World's forests 2009. Report 117, Food and Agriculture Organization of the United Nations, Rome.
Farnsworth, K.L., Milliman, J.D., 2003. Effects of climate and anthropogenic change on small mountainous rivers: the Salinas River example. Global Planet. Change 39, 53–64.
Farr, T.G., Rosen, P.A., Caro, E., Crippen, R., Duren, R., Hensley, S., Kobrick, M., Paller, M., Rodriguez, E., Roth, L., Seal, D., Shaffer, S., Shimada, J., Umland, J., Werner, M., Oskin, M., Burbank, D., Alsdorf, D., 2007. The shuttle radar topography mission. Rev. Geophys. 45, RG2004. doi:10.1029/2005RG000183.
Galloway, W.E., 1975. Process framework for describing the morphologic and stratigraphic evolution of deltaic depositional systems. In Broussard, M.L. (Ed.), Deltas: Models for Exploration. Houston Geological Society, Houston, TX, pp. 87–96.
Giraldo, A., Rodríguez-Rubio, E., Zapata, F., 2008. Oceanographic conditions off Gorgona Island, eastern tropical Pacific of Colombia. Latin Am. J. Aquat. Res. 36, 121–128.
Gómez, H., 1986a. Contribución geomorfológica y estructural del suroccidente colombiano y de la costa pacífica entre Tumaco-Buenaventura y Quibdo. CIAF, Bogotá. 33.
Gómez, H., 1986b. Algunos aspectos neotectónicos hacia el suroeste del Litoral Pacífico colombiano. Rev. CIAF 11, 281–289.
González, J.L., Correa, I.D., Aristizábal, O., 2002. Evidencias de subsidencia cosísmica en el delta del San Juan. In: Correa, I.D., Restrepo, J.D. (Eds.), Geología y Oceanografía del delta del río San Juan: Litoral Pacífico Colombiano. Fondo Editorial Universidad EAFIT, Medellín, pp. 89–110.
Harden, C.P., 2006. Human impacts on headwater fluvial systems in the northern and central Andes. Geomorphology 79, 249–263.

Herd, D.G., Youd, T.L., Meyer, H., Arango, J.L., Person, W.J., Mendoza, C., 1992. The great Tumaco, Colombia earthquake of December 1979. Science 211, 441–445.
HIDROSIG, 2006. Balances Hidrológicos de Colombia. Postgrado en Aprovechamiento de Recursos Hidráulicos, Universidad Nacional (Sede Medellín), software (version 1.8).
Hood, W.G., 2010. Delta distributary dynamics in the Skagit River Delta (Washington, USA): extending, testing, and applying avulsion theory in a tidal system. Geomorphology doi:10.1016/j.geomorph.2010.07.007.
Hovius, N., Stara, C.P., Allen, P.A., 1997. Sediment flux from a mountain belt derived by landslide mapping. Geology 25, 231–234.
Hovius, N., 1998. Controls on sediment supply by large rivers. In: Shanley, K.W., McCabe, P.J. (Eds.) Relative role of Eustasy, Climate, and Tectonism in Continental Rocks. SEPM Special Publication 59, Tulsa, OK, pp. 3–16.
IDEAM, 2007. Datos Horarios del nivel relativo del mar para la estación mareográfica de Tumaco, 1953–2006. Instituto de Hidrología, Meteorología y Estudios Ambientales IDEAM. Digital format.
IDEAM, 2009 (Data). River Database of the Patía drainage basin. Instituto de Hidrología, Metereología y Estudios Ambientales (IDEAM), Bogotá, Colombia (5 gauging stations).
INGEOMINAS, 2007. Sismicidad registrada por la Red Sismológica Nacional de Colombia (Junio de 1993 a Septiembre de 2007), Mapa del Pacífico sur colombiano. Ingeominas, Bogotá.
IPCC, 2001. Climate change 2001: Impacts, Adaptation, and Vulnerability. Tech. Rep., Intergovernmental Panel of Climate Change.
Kellogg, J.N., Mohriak, W.U., 2001. The tectonic and geological environment of coastal South America. In: Seeliger, U., Kjerfve, B. (Eds.), Coastal Marine Ecosystems of Latin America. Springer Verlag, Berlin-Heidelberg, pp. 2–16.
Latrubesse, E.M., Stevaux, J.C., Sinha, R., 2005. Tropical rivers. Geomorphology 70, 187–206.
Lockridge, P.A., Smith, R.H., 1984. Tsunamis in the Pacific Basin 1900–1983: Map (1:17, 000.000). National Geophysical Data Center, Boulder, Colorado.
López, S.A., Restrepo, J.D., Restrepo, J.C., Monroy, C., Mora, H., Rubio, E., 2009. Nivel relativo del mar en la costa pacífica sur de Colombia: variabilidad, tendencias e implicaciones en la dinámica deltaica. Boletín Geológico 42, 53–66.
Martínez, J.O., González, J.L., Pilkey, O.H., Neal, W.J., 1995. Tropical barrier islands of Colombia's Pacific coast. J. Coastal Res. 11, 432–453.
Meade, R.H., 1988. Movement and storage of sediment in river systems. In: Lerman, A., Meybeck, M. (Eds.), Physical and Chemical Weathering in Geochemical Cycles. North American Treaty Organization Advanced Scientific Series C Mathematical and Physical Sciences. Kluwer, Pandraht, pp. 165–180.
Meyer, H., Mejía, J.A., Velásquez, A., 1992. Informe preliminar sobre el terremoto del 19 de noviembre de 1991 en el Departamento del Chocó. Publicaciones Ocasionales OSSO, Universidad del Valle, Cali, Colombia, 13.
Milliman, J.D., Syvitski, P.M., 1992. Geomorphic/tectonic control of sediment transport to the ocean: the importance of small mountainous rivers. J. Geol. 100, 525–544.
Morgan, R.P.C. (Ed.), 1986. Soil Erosion and Conservation. Longman, Harlow.
Morton, R.A., González, J.L., López, G.I., Correa, I.D., 2000. Frequent non-storm washover of barrier islands, Pacific coast of Colombia. J. Coastal Res. 16, 82–87.
Oldeman, L.R., Hakkeling, R.T.A., Sombroek, W.G. (Eds.), 1991. World Map of the Status of Human-Induced Soil Degradation: An Explanatory Note. ISRIC, Wageningen.
Orozco, L., 2004. Propuesta de definición de provincias sismotectónicas y modelo de bloques de deformación actual para Colombia. Convenio Marco de Cooperación INGEOMINAS – Universidad de Caldas. INGEOMINAS. Bogotá. 189.
Overeem, I., Syvitski, J.P.M., 2009. Dynamics and Vulnerability of Delta Systems. LOICZ Reports & Studies No. 35. GKSS Research Center, Geesthacht, 54.
Pennington, W.D., 1981. Subduction on the eastern Panama Basin and seismotectonics of Northwestern South America. J. Geophys. Res. 86, 10753–10770.
Penland, S., Kulp, M.A., 2005. Deltas. In: Schwartz, M. (Ed.), Encyclopedia of Coastal Science. Springer, pp. 362–386.
Quinn, W.H., Zopf, D.O., Short, K.S., Kuo Yang, R.T.W., 1978. Historical trends and statistics of the Southern Oscillation, El Niño and Indonesian droughts. Fish. Bull. 76, 663–678.
Restrepo, J.D., Kjerfve, B., 2000. Water discharge and sediment load from the western slopes of the Colombian Andes with focus on Rio San Juan. J. Geol. 108, 17–33.
Restrepo, J.D., Kjerfve, B., 2002. San Juan River delta, Colombia: tides, circulation, and salt dispersion. Cont. Shelf Res. 22, 1249–1267.
Restrepo, J.D., Kjerfve, B., Correa, I.D., González, J.L., 2002. Morphodynamics of a high discharge tropical delta, San Juan River, Pacific coast of Colombia. Marine Geol. 192, 355–381.
Restrepo, J.D., Syvitski, J.P.M., 2006. Assessing the Effect of Natural Controls and Land Use Chane on Sediment Yield in a Major Andean River: the Magdalena Drainage Basin, Colombia. Ambio: J. Human Environ. 35, 44–53.
Restrepo, J.D., López, S.A., 2008. Morphodynamics of the Pacific and Caribbean Deltas of Colombia, South America. J. South Am. Earth Sci. 25, 1–21.
Sánchez-Triana, E., Ahmed, K., Awe, Y., 2007. Prioridades ambientales para la reducción de la pobreza en Colombia: un análisis ambiental del país para Colombia. Informe del Banco Mundial, Direcciones para el Desarrollo, medio ambiente y desarrollo sustentable. Report No. 38610. Washington, DC, 522.
Soeters, R., Gómez, J., 1985. Contribución del studio geomorfológico para el proyecto de canales y esteros. In Rizo, D., Contreras, R. (Eds.), Estudio del impacto ambiental para la proyección y canalización de esteros. Corporación Valle del Cauca-Plan de Adecuación de Esteros y Canales, Cali, pp. 285–337.
Stallard, R.F., 1988. Weathering and erosion in the humid Tropics. In: Lerman, A., Meybeck, M. (Eds.), Physical and Chemical Weathering in Geochemical Cycles. North American Treaty Organization Advanced Scientific Series C Mathematical and Physical sciences. Kluwer, Pandraht, pp. 225–246.
Syvitski, J.P.M., 2003. Supply and flux of sediment along hydrological pathways: research for the 21st century. Global Planet. Change 39, 1–11.
Syvitski, J.P.M., Kettner, A.J., Overeem, I., Hutton, E.W.H., Hannon, M.T., Brakenridge, G.R., Day, J., Vorosmarty, C., Saito, Y., Giosan, L., Nicholls, R.J., 2009. Sinking deltas due to human activities. Nat. Geosci. 2, 681–686.
Tavera, H.A., 2009. Documentos síntesis. Proyecto caracterización, diagnóstico y zonificación de los manglares en el departamento de Nariño. Ministerio de Ambiente, Vivienda y Desarrollo Territorial, Corporación Autónoma Regional de Nariño y World Wide Found for Nature-WWF Colombia. Bogotá, 50.
Thieler, E.R., Himmelstoss, E.A., Zichichi, J.L., Miller, T.L., 2005. Digital Shoreline Analysis System (DSAS) version 3.0: an ArcGIS extension for calculating shoreline change. US Geolological Survey Open. File Report, 2005-1304.
Thom, B.G., 1967. Mangrove ecology and deltaic geomorphology, Tabasco, Mexico. J. Ecol. 55, 301–343.
Tolman, H.L., 2002. Validation of WAVEWATCHIII Version 1.15 for a Global Domain. Technical Note, National Oceanic and Atmospheric Administration-National Weather Service, Washington, DC, 33.
UNODC (United Nation Office Against Drugs), 2009. Colombia: Censo de cultivos de coca. Oficina de las Naciones Unidas contra la Droga y el Delito, Bogotá, Colombia, 107.
US Department of State, 2001. The Andes under Siege; Environmental consequences of the drug trade. <http://usinfo.state.gov/products/pubs/archive/>.
Vann, J., 1959. Landform-vegetation relationships in the Atrato delta. Ann. Ass. Am. Geogr. 49, 345–360.
Velásquez, A., Meyer, H., Marin, W., Ramirez, F., Drews, A.D., Campos, A., Hermelin, M., Bender, S., Arango, M., Serje, J., 1994. Planificación regional del occidente colombiano bajo la consideración de las restricciones por amenazas. Memorias del Taller OEA sobre planificación del desarrollo regional y prevención de desastres, Spec. Publ., pp 1–36.
Walling, D.E., Fang, D., 2003. Recent trends in the suspended sediment loads of the world's rivers. Global Planet. Change 39, 111–126.
Wright, L.D., Coleman, J.M., 1971. Effluent expansion and interfacial mixing in the presence of a salt wedge, Mississippi River delta. J. Geophys. Res. 76, 8649–8661.